Saccharomyces cerevisiae Replication Protein A Binds to Single-Stranded DNA in Multiple Salt-Dependent Modes†

Sangaralingam Kumaran, Alexander G. Kozlov, and Timothy M. Lohman*

Department of Biochemistry and Molecular Biophysics, Washington University School of Medicine, 660 South Euclid Avenue, St. Louis, Missouri 63110

Received May 18, 2006; Revised Manuscript Received July 19, 2006

ABSTRACT: We have examined the single-stranded DNA (ssDNA) binding properties of the *Saccharomyces cerevisiae* replication protein A (scRPA) using fluorescence titrations, isothermal titration calorimetry, and sedimentation equilibrium to determine whether scRPA can bind to ssDNA in multiple binding modes. We measured the occluded site size for scRPA binding poly(dT), as well as the stoichiometry, equilibrium binding constants, and binding enthalpy of scRPA−$(dT)_L$ complexes as a function of the oligodeoxynucleotide length, *L*. Sedimentation equilibrium studies show that scRPA is a stable heterotrimer over the range of [NaCl] examined (0.02−1.5 M). However, the occluded site size, *n*, undergoes a salt-dependent transition between values of $n = 18-20$ nucleotides at low [NaCl] and values of $n = 26-28$ nucleotides at high [NaCl], with a transition midpoint near 0.36 M NaCl (25.0 °C, pH 8.1). Measurements of the stoichiometry of scRPA−$(dT)_L$ complexes also show a [NaCl]-dependent change in stoichiometry consistent with the observed change in the occluded site size. Measurements of the ΔH_{obsd} for scRPA binding to $(dT)_L$ at 1.5 M NaCl yield a contact site size of 28 nucleotides, similar to the occluded site size determined at this [NaCl]. Altogether, these data support a model in which scRPA can bind to ssDNA in at least two binding modes, a low site size mode ($n = 18 \pm 1$ nucleotides), stabilized at low [NaCl], in which only three of its oligonucleotide/oligosaccharide binding folds (OB-folds) are used, and a higher site size mode ($n = 27 \pm 1$ nucleotides), stabilized at higher [NaCl], which uses four of its OB-folds. No evidence for highly cooperative binding of scRPA to ssDNA was found under any conditions examined. Thus, scRPA shows some behavior similar to that of the *E. coli* SSB homotetramer, which also shows binding mode transitions, but some significant differences also exist.

Single-stranded (ss) DNA binding (SSB) proteins exist in nearly all organisms and play central roles in all aspects of DNA metabolism, including DNA replication, repair, and recombination. However, the structural forms of SSB proteins differ considerably among different organisms. For example, the bacteriophage T4 gene 32 protein, the first such SSB protein identified (*1*, *2*) is a monomer, whereas the *Escherichia coli* SSB protein is a homotetramer (*3*, *4*), as are most SSB proteins from eubacteria. In contrast, the eukaryotic SSB protein, commonly called replication protein A (RPA), is a heterotrimer (*5*, *6*).

In all eukaryotes, RPA consists of three highly conserved subunits of approximately 70, 32, and 14 kDa, named according to their respective molecular masses, and all three subunits are required for function in vivo (*5*, *6*). However, RPA homologues display distinct species specificity, such that scRPA[1] from yeast cannot substitute for human RPA (hsRPA) in cell-free SV40 replication assays (*7*, *8*). These specificities presumably reflect the fact that RPA proteins also are involved in myriad interactions with other proteins. These include DNA polymerase α (*9*), XPA (*10*), XPG (*11*), XPF-ERCCI (*12*), proteins in the Rad52 epistasis group (*13*), and the Blooms (*14*) and Werner helicases (*15*), as well as many others (*16*−*19*).

Although SSB proteins from different organisms can differ in architecture, one common feature is that the sites for ssDNA binding consist primarily of so-called oligonucleotide/oligosaccharide binding folds (OB-folds) (*20*). Whereas T4 gene 32 protein contains one OB-fold, the *E. coli* SSB tetramer contains four OB-folds and the heterotrimeric RPA contains six OB-folds. Each OB-fold within RPA could potentially provide a site for ssDNA binding (*21*−*24*). Four OB-folds are located within RPA70, referred to as F, A, B, and C (see Figure 1), a fifth OB-fold (D) is contained within the RPA32 subunit, and a sixth OB-fold (E) is contained within RPA14.

The ssDNA binding properties of RPA have previously been characterized using a variety of approaches (*25*−*29*). As is true for most SSB proteins, RPA binds with high affinity to ssDNA with no apparent sequence specificity (*26*, *29*−*32*), although it does display a preference for polypyrimidines (*26*). The primary sites on RPA that interact with ssDNA have been mapped to the central part of the RPA70 subunit (OB-folds A and B) (*21*, *33*−*35*), whereas the

† This research was supported in part by the NIH (Grant RO1 GM30498).

* To whom correspondence should be addressed. E-mail: lohman@biochem.wustl.edu. Phone: (314) 362-4393. Fax: (314) 362-7183.

[1] Abbreviations: scRPA, yeast single-stranded DNA binding protein; ssDNA, single-stranded DNA; OB-fold, oligonucleotide/oligosaccharide binding fold; ITC, isothermal titration calorimetry; Tris, tris(hydroxymethyl)aminomethane; HEPES, 4-(hydroxyethyl)-1-piperazineethanesulfonic acid; EDTA, ethylenediaminetetraacetic acid.

10.1021/bi060994r CCC: $33.50
Published on Web 09/09/2006

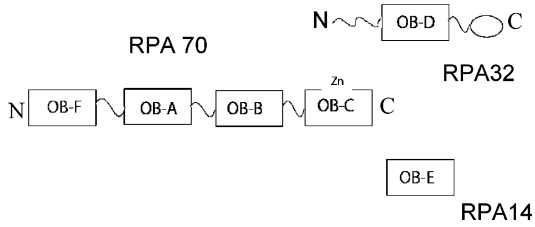

FIGURE 1: Schematic representation of the scRPA heterotrimer with its six OB-folds. Four OB-folds are contained within RPA70 (OB-folds A, B, C, and F), one is contained within RPA32 (OB-fold D), and one is contained within RPA14 (OB-fold E).

N-terminal OB-fold of RPA70 participates in protein−protein interactions (*9*). There is no evidence that the OB-fold of RPA14 (OB-fold E) has DNA binding activity (*36*, *37*). There is however evidence that OB-fold D in RPA32 can interact with ssDNA, although this depends on the length of the ssDNA oligodeoxynucleotide (*27*) as well as the solution conditions (*37*).

The *E. coli* SSB tetramer, which contains four OB-folds (one per subunit), can bind to ssDNA using either two subunits in its $(SSB)_{35}$ mode (highly cooperative binding mode with an occluded site size of 35 nucleotides) or all four subunits in its $(SSB)_{65}$ mode (low cooperative binding mode with an occluded site size of 65 nucleotides) depending on the solution conditions (*3*, *4*, *38*−*42*), and the transition between these modes depends on the salt concentration and type, temperature, and pH (*39*, *43*−*45*). By analogy with *E. coli* SSB, it has been suggested that RPA might also bind in various "binding modes" differing in the number of OB-folds that interact with the ssDNA (*37*, *46*). Some support for this proposal has come from mutagenesis studies (*27*) with short oligodeoxynucleotides; however, there is little evidence suggesting that RPA can bind to long ssDNA in multiple binding modes or that RPA might undergo transitions among alternative binding modes in solution.

The binding site size of RPA when bound to ssDNA has been measured for RPA from a variety of species, with variable results depending on the approach used, but also the species. There appears to be general agreement for the binding site size of hsRPA on ssDNA (30 nucleotides) (*25*, *28*), although a less stable mode involving interactions with only 8−10 nucleotides of ssDNA, which is observable only upon cross-linking, has also been reported (*28*). A site size of 22 nucleotides has been reported for *Drosophila melanogaster* (dm) RPA (*32*), 20−25 nucleotides for calf thymus RPA (*30*), and 20−30 nucleotides for RPA from primates (*47*). However, the reported site sizes for yeast scRPA binding to ssDNA vary over a much wider range from 20 to 90 nucleotides (*29*, *48*, *49*). Furthermore, there is evidence suggesting that the ssDNA binding properties of hsRPA and scRPA differ in detail (*48*). Finally, there seems to be no consensus on the site sizes that characterize any of the proposed different binding modes (*27*, *50*, *51*).

One difficulty in assessing whether the range of RPA binding site sizes reported reflects true differences is that these studies used a variety of different approaches and were performed under different solution conditions. Since the *E. coli* SSB tetramer in complex with ssDNA has been shown to undergo a salt-dependent binding mode transition (*39*, *52*), it is possible that some of the variability observed for the scRPA binding site size is due to differences in the solution conditions used. We have therefore undertaken a systematic study to examine whether scRPA binds to ssDNA in different binding modes using the same approaches (fluorescence, isothermal titration calorimetry, and analytical sedimentation) previously used to examine the *E. coli* SSB protein.

MATERIALS AND METHODS

Reagents and Buffers. All buffers were prepared from reagent-grade chemicals using doubly distilled water that was further deionized using a Milli-Q purification system. (Millipore Corp., Bedford, MA). Buffer T is 10 mM Tris (pH 8.1), 0.1 mM Na_3EDTA. The filter binding buffer is 30 mM HEPES (pH 7.8), 5 mM $MgCl_2$, 100 mM NaCl, 0.5% inositol (w/v), 1 mM dithiothreitol.

scRPA Protein and Nucleic Acids. The expression vector p11d-sctRPA encoding the genes for all three subunits of scRPA (generous gift from Dr. Marc S. Wold, University of Iowa) was used to transform *E. coli* BL21(DE3) cells. The scRPA heterotrimer was expressed and purified as described (*48*) with the following modification. scRPA was eluted from the anion exchange column (Mono-Q 5/50 GL, Pharmacia) using a 10 mL linear gradient from 100 to 400 mM KCl. scRPA elutes at ∼300 mM KCl with a yield of 0.8−1.0 mg/L of culture. We also included a single-stranded DNA cellulose column as an additional purification step to be sure that all RPA used in our experiments has ssDNA binding activity. The ssDNA cellulose column was equilibrated with buffer T + 0.3 M NaCl before the protein was loaded. The protein that eluted from the Mono-Q column was diluted 2-fold with buffer T + 0.02 M NaCl before being loading onto the ssDNA column. The ssDNA column was washed successively with buffer T + 0.3 M NaCl and buffer T + 0.5 M NaCl, and the scRPA was eluted with buffer T + 2.0 M NaCl + 10% (v/v) glycerol. The purity of scRPA was >98%, judged by SDS−polyacrylamide gel electrophoresis. The purified protein was dialyzed into buffer T + 0.1 M NaCl, 0.2 mM 2 mercaptoethanol, and 30% (v/v) glycerol and stored at −20 °C. The scRPA concentration was determined spectrophotometrically in buffer T (0.02 M NaCl) by using an extinction coefficient of 9.85×10^4 M^{-1} cm^{-1} (*48*).

The oligodeoxynucleotides, $(dT)_L$, were synthesized and purified as described (*41*) and were ≥98% pure as judged by denaturing gel electrophoresis. The 5′-Cy3-$(dT)_{29}$ used for sedimentation studies was further purified by reversed-phase HPLC using an Xterra MS C18 column (Waters, Milford, MA). The poly(dT) (Midland Certified Reagent Co., Midland, TX (catalog no. P-2004, lot no. 040495)) had an average length of ∼1100 nucleotides. All DNA samples were dissolved in buffer T and dialyzed extensively before use. Single-stranded circular M13 mp18 DNA was purchased from New England Biolabs (catalog no. N4040S, lot no. 11) and was supplied in 10 mM Tris−HCl (pH 7.5), 1 mM EDTA. Concentrations of the nucleic acids were determined spectrophotometrically using the extinction coefficients: $(dT)_L$ and poly(dT), $\epsilon_{260} = 8.1 \times 10^3$ M^{-1} (nucleotide) cm^{-1} (*53*); single-stranded M13 DNA, $\epsilon_{259} = 7370$ M^{-1} (nucleotide) cm^{-1} (*54*); Cy3-$(dT)_{29}$, $\epsilon_{260} = 2.4 \times 10^5$ M^{-1} cm^{-1}, calculated as described (*55*).

Analytical Ultracentrifugation. Sedimentation equilibrium and velocity experiments were performed using an Optima

Table 1: Molecular Mass Determined for scRPA by Sedimentation Equilibrium Experiments at 25° C

buffer conditions	expected molecular mass (kDa)	obsd molecular mass (kDa)
buffer T + 20 mM NaCl	114	115 ± 5
buffer T + 1.0 M NaCl	114	119 ± 3
buffer T + 1.5 M NaCl	114	122 ± 4
buffer T + 0.2 M NaCl + 10% glycerol	114	118 ± 3

XL-A analytical ultracentrifuge and an An50Ti rotor (Beckman Instruments, Inc., Fullerton, CA). All samples were dialyzed extensively versus buffer T containing the indicated amount of salt. Sedimentation equilibrium experiments were performed at three different protein concentrations (120 μL) using an Epon charcoal-filled six-channel centerpiece. Experiments were also usually performed at three rotor speeds starting with the slowest rotor speed. Samples were scanned at a wavelength of 280 nm, and data were collected at a spacing of 0.001 cm with an average of seven scans per step. Attainment of equilibrium was judged by overlaying at least three successive scans taken at 2 h intervals. Data sets were edited with WinREEDIT (http://www.biotech.uconn.edu/auf/) to extract the data between the meniscus and the bottom of the cell and were then analyzed by nonlinear least squares (NLLS) methods using WINNONLIN (David Yphantis, University of Connecticut; Michael Johnson, University of Virginia; Jeff Lary, National Analytical Ultracentrifuge Center, Storrs, CT) and SCIENTIST (Micromath, St. Louis, MO).

Apparent molecular weights were obtained by fitting the sedimentation equilibrium data to the eq 1:

$$A_T = \sum_{i=1}^{n} \exp(\ln A_{0,i} + \sigma_i(r^2 - r_{ref}{}^2)/2) + b \qquad (1)$$

where A_T is the total absorbance at radial position r, $A_{0,i}$ is the absorbance of component i at the reference radial position (r_{ref}), b is the baseline offset, $\sigma_i = [M_i(1 - \bar{\upsilon}_i\rho)\omega^2]/RT$, M_i is the molecular mass of component i, $\bar{\upsilon}_i$ is the partial specific volume of component i, ρ is the solution density (calculated using SEDNTREP (David Hayes, Magdalen College; Tom Laue, University of New Hampshire; John Philo, Amgen), ω is the angular velocity, R is the ideal gas constant, and T is the absolute temperature. A global NLLS fit of the absorbance profiles to eq 1 returns M for each component present at equilibrium, providing $\bar{\upsilon}_i$ is known. For scRPA, $\bar{\upsilon}_i$ was calculated from its amino acid composition using the program SEDNTREP, yielding 0.7294 mL g^{-1} at 25 °C; $\bar{\upsilon}_i$ for Cy3(dT)$_{29}$ was 0.58 mL g^{-1} (*56*). Sedimentation equilibrium→experiments performed at three different protein concentrations, in buffer T + 200 mM NaCl + 10% (v/v) glycerol, were fit to eq 1 using a $\bar{\upsilon}_i$ value of 0.7294 mL g^{-1}, and the values of M are listed in Table 1. The calculated values of $\bar{\upsilon}_i$ were corrected for the presence of 10% (v/v) glycerol as described (*57*). The corrected value of $\bar{\upsilon}_i$ is 0.7327 ± 0.0016 mL g^{-1}. Cy3-(dT)$_{29}$ alone in buffer T sediments as a single species with M_{app} = 9.8 ± 0.2 kDa, close to the expected value of 9.3 kDa. For the NLLS analysis of protein−DNA complexes, σ_{DNA} was fixed to the value determined independently for DNA, while $\sigma_{protein-DNA}$ floated. The values of $\bar{\upsilon}$ for the protein−DNA complexes were calculated as the weight-average sum of $\bar{\upsilon}$ for the individual components, as in the eq 2:

$$\bar{\upsilon}_{RnD} = \frac{nM_{Rf}\bar{\upsilon}_{Rf} + M_{Df}\bar{\upsilon}_{Df}}{nM_{Rf} + M_{Df}} \qquad (2)$$

where $\bar{\upsilon}_{RnD}$ is the partial specific volume for the protein−DNA complex, M_{Rf} and M_{Df} are the molecular masses of scRPA and the DNA substrate (g mol^{-1}), and $\bar{\upsilon}_{Rf}$ and $\bar{\upsilon}_{Df}$ are the partial specific volumes of scRPA and the DNA substrate, respectively (mL g^{-1}). The sedimentation velocity experiments were analyzed using the program DCDT$^+$ (version 1.16, John S. Philo) to obtain estimates of the molecular masses.

Fluorescence Measurements. Titrations of scRPA with ssDNA were performed by monitoring the intrinsic tryptophan fluorescence of scRPA using a PTI QM-4 spectrofluorometer (Photon Technology International, Lawrenceville, NJ) equipped with a 75 W Xe lamp. The excitation wavelength was 295 nm, and the fluorescence intensity was monitored at 345 nm. All slit widths were set to 0.5 mm, and photobleaching under these conditions was less than 2%. The sample temperature was controlled at 25.0 ± 0.2 °C using a Lauda RM6 recirculation water bath (Brinkmann, Westbury, NY). A 1.9 mL solution of scRPA in a 4.0 mL quartz cuvette (10 mm path length, 3 mL) (NSG Precision Cells Inc., Farmingdale, NY) was equilibrated with constant stirring using an 8 mm diameter cylindrical cell stirrer (P-73 from NSG Precision Cells, Inc.) for at least 30 min until the tryptophan fluorescence intensity reached a constant value. Initial readings of both the sample, $F_{samp,0}$, and reference (containing only buffer), $F_{ref,0}$, cuvettes were then taken, with $F_0 = F_{samp,0} - F_{ref,0}$ defined as the initial fluorescence of the sample. The sample cuvette was then titrated with aliquots of DNA, and the solution was equilibrated for 3 min with stirring. For each point in the titration, the sample was excited for 10 s, during which five data points were taken, after which the shutter was closed. Data points from two such measurements were averaged to obtain $F_{samp,i}$, the fluorescence intensity after the ith addition of DNA. A second cuvette containing buffer was also titrated with DNA, yielding the background fluorescence, $F_{ref,i}$. The difference between these two readings is defined as the observed fluorescence for each titration point i, $F_{obsd,i} = F_{samp,i} - F_{ref,i}$. The relative fluorescence quenching upon DNA binding is defined as $Q_{obsd,i} = (F_0 - F_{obsd,i})/F_0$. All measurements were corrected for dilution and inner filter effects as described (*58*).

Model-Independent Determination of Binding Isotherms and Stoichiometries of scRPA−ssDNA Complexes. The binding of oligodeoxythymidylates, $(dT)_L$, to scRPA was monitored by the quenching of the intrinsic tryptophan fluorescence of the protein, Q_{obsd}. Model-independent estimates of the average number of moles of $(dT)_L$ bound per mole of scRPA heterotrimer, $\sum\Theta_i$, were obtained using the binding density function method (*59*). The observed fluorescence quenching of the scRPA protein at any point in the titration is related to $\sum\Theta_i$ by eq 3:

$$Q_{obsd} = \sum \Theta_i Q_{i_{max}} \qquad (3)$$

where $Q_{i_{max}}$ is the extent of fluorescence quenching when a

$(dT)_L$ molecule is bound to site *i*. Since each $Q_{i_{max}}$ is constant for a given state *i*, then at equilibrium Q_{obsd} is dependent only upon the distribution of $(dT)_L$ bound. Therefore, at any constant value of Q_{obsd}, the value of $\sum\Theta_i$ is also constant. Hence, from titrations (Q_{obsd} versus log D_{tot}) performed at two (or more) different concentrations of scRPA protein, $R_{tot,1}$ and $R_{tot,2}$, one can determine the set of values of the concentrations of total nucleic acid, $D_{tot,1}$ and $D_{tot,2}$, for which Q_{obsd} is constant, and thus $\sum\Theta_i$ can be calculated from eq 4:

$$\sum\Theta_i = \frac{D_{tot,2} - D_{tot,1}}{R_{tot,2} - R_{tot,1}} \quad (4)$$

Analysis of Fluorescence Titrations for the Binding of Short $(dT)_L$ ($L \leq n$) to scRPA. Binding of $(dT)_L$ to scRPA with $L = 20$, 22, 26, and 28 nucleotides (1.5 M NaCl) was analyzed to obtain the equilibrium binding constant, K_{obsd} = [RD]/[R][D], using a single-site binding model described in eq 5a:

$$\frac{Q_{obsd}}{Q_{max}} = \frac{K_{L,obsd}D}{1 + K_{L,obsd}D} \quad (5a)$$

where Q_{obsd} is the observed fluorescence quenching and Q_{max} is the maximum fluorescence quenching observed at saturation of the scRPA (R) with $(dT)_L$ (D) to form RD. *D* can be found from the mass conservation eq 5b:

$$D_{tot} = D + D_{bound} = D + \frac{K_{L,obsd}D}{1 + K_{L,obsd}D}R_{tot} \quad (5b)$$

The binding of two $(dT)_{18}$ molecules to scRPA at high salt concentration was analyzed using a two-site binding model described in eq 6a:

$$Q_{obsd} = \frac{Q_1,K_{1,obsd}D + (Q_1 + Q_2)K_{1,obsd}K_{2,obsd}D^2}{1 + K_{1,obsd}D + K_{1,obsd}K_{2,obsd}D^2} \quad (6a)$$

where Q_{obsd} is the observed fluorescence quenching, Q_1 and Q_2 are the fluorescence quenchings corresponding to the first and the second $(dT)_L$ molecule bound, respectively, and $K_{1,obsd}$ and $K_{2,\ obsd}$ are the stepwise association constants for the binding of the first and the second DNA molecules ($K_{1,obsd}$ = [RD]/[R][D] and $K_{2,obsd}$ = $[RD_2]$/[RD][D]). The concentration of free DNA, *D*, was determined from the mass conservation eq 6b:

$$D_{tot} = D + D_{bound} = D + \frac{K_{1,obsd}D + 2K_{1,obsd}K_{2,obsd}D^2}{1 + K_{1,obsd}D + K_{1,obsd}K_{2,obsd}D^2}R_{tot} \quad (6b)$$

Fitting of the data to the models in eqs 5a and 6a was performed using SCIENTIST (Micromath Research, St. Louis MO).

Isothermal Titration Calorimetry (ITC). ITC experiments were performed in buffer T (25 °C) at three [NaCl] (0.02, 0.2, and 1.5 M), using a VP-ITC calorimeter (Microcal, Northampton, MA) as described (*60*). Both the scRPA (R) and $(dT)_L$ (D) were dialyzed extensively versus reaction buffer. All samples and buffer solutions were degassed at room temperature prior to use. Most experiments were carried out by titrating scRPA (0.25−1.0 μM) with $(dT)_L$ (5−15 μM), although one experiment at 0.2 M NaCl was performed by titrating $(dT)_L$ (0.43 μM) with scRPA (21.1 μM). Control experiments to determine the heat of dilution for each injection were performed by injecting the same volumes of $(dT)_L$ (or scRPA) into the sample cell containing only buffer.

The data obtained in 1.5 M NaCl (see Figures 4A and 8) were analyzed using a 1:1 binding model described by eq 7a:

$$Q_i^{tot} = V_0\Delta HR_{tot}\frac{K_{obsd}D}{1 + K_{obsd}D} \quad (7a)$$

where Q_i^{tot} is the total heat after the *i*th injection, V_0 is the volume of the calorimetric cell, and K_{obsd} and ΔH are the observed equilibrium binding constant (K_{obsd} = [RD]/[R][D]) and corresponding enthalpy change. The concentration of free $(dT)_L$, *D*, was obtained from eq 7b:

$$D_{tot} = D + D_{bound} = D + R_{tot}\frac{K_{obsd}D}{1 + K_{obsd}D} \quad (7b)$$

In eqs 7a and 7b, D_{tot} and R_{tot} are the total concentrations of the ssDNA and scRPA in the calorimetric cell after the *i*th injection. To obtain the binding parameters K_{obsd} and ΔH, the experimental data were fit to this model using software provided by the instrument manufacturer. The details of the conversion of integral heats (Q_i^{tot}) to differential heats (heats per injection observed in the experiment) and the fitting routine including corrections for heat displacement effects and DNA and protein dilutions in the cell are described in the *ITC Data Analysis in Origin Tutorial Guide* (Microcal Inc.) and ref *60*.

At 0.02 and 0.2 M NaCl, a single $(dT)_{30}$ molecule can bind two molecules of scRPA (see Figure 4B−D). Equilibrium binding under these conditions was analyzed using a two-site sequential model, such that the total heat (Q_i^{tot}) after the *i*th injection is defined by eq 8a:

$$Q_i^{tot} = V_0D_{tot}\frac{\Delta H_1K_{1,obsd}R + (\Delta H_1 + \Delta H_2)K_{1,obsd}K_{2,obsd}R^2}{1 + K_{1,obsd}R + K_{1,obsd}K_{2,obsd}R^2} \quad (8a)$$

where $K_{1,obsd}$, ΔH_1 and $K_{2,obsd}$, ΔH_2 are the observed stepwise macroscopic equilibrium constants ($K_{1,obsd}$ = [DR]/[D][R] and $K_{2,obsd}$ = $[DR_2]$/[DR][R]) and enthalpy changes for binding of the first and second molecules of scRPA to $(dT)_{30}$, respectively. *R* is the free scRPA concentration, which can be found using eq 8b:

$$R_{tot} = R + R_{bound} = R + D_{tot}\frac{K_{1,obsd}R + 2K_{1,obsd}K_{2,obsd}R^2}{1 + K_{1,obsd}R + K_{1,obsd}K_{2,obsd}R^2} \quad (8b)$$

The binding parameters $K_{1,obsd}$, ΔH_1 and $K_{2,obsd}$, ΔH_2 were obtained by fitting the experimental data to this model using software provided by the instrument manufacturer as described in the *ITC Data Analysis in Origin Tutorial Guide* (Microcal Inc.) and by Kozlov and Lohman (*60*).

Agarose Gel Electrophoresis. Agarose gel electrophoresis to examine the cooperativity of scRPA−ssM13 DNA

complexes was performed as described (*61*) using 0.5% agarose gels (14 cm horizontal gels). The total reaction volume of each sample was 30 μL. In a series of experiments, the DNA concentration was held constant (0.5 μg), while the scRPA concentration was varied. The solution conditions used are given in the text for each experiment. The gel electrophoresis running buffer was 20 mM Tris (pH 7.8), 0.4 mM sodiumacetate, 0.2 mM Na_3EDTA. Loading dye (2 μL of 50% (v/v) glycerol, 0.04% (w/v) bromophenol blue) was added to each 30 μL sample. Electrophoresis was carried out at room temperature (22 °C) at constant voltage (8 V/cm) for 3−3.5 h. The gels were then stained for 15 min with ethidium bromide (2 μg/mL solution) and destained for 2−3 h at 4 °C in buffer T + 2 M NaCl.

RESULTS

Stability of the scRPA Heterotrimer. To facilitate interpretation of our scRPA−ssDNA binding studies, we first examined the assembly state of the protein under the solution conditions used to examine DNA binding. Both sedimentation equilibrium and sedimentation velocity experiments were performed as described in the Materials and Methods at five NaCl concentrations (20 mM, 0.2 M, 1.0 M, 1.5 M, and 2.5 M) in buffer T at 25 °C. The results of sedimentation equilibrium experiments performed in 20 mM and 1.5 M NaCl are shown in parts A and B, respectively, of Figure 2. All sedimentation equilibrium data were analyzed globally using NLLS methods, and all sedimentation profiles obtained at [NaCl] ≤ 1.5 M were well described by a model for a single ideal species (eq 1 with $n = 1$; see the Materials and Methods) with average molecular masses close to that expected for an scRPA heterotrimer ($M_r = 114000$ Da) (see Table 1). In sedimentation velocity experiments performed in buffer T plus 20 mM NaCl at 25 °C (data not shown) ([scRPA] = 1.2 μM), scRPA sediments as a single species with a weight average sedimentation coefficient $\bar{S}_{20,w} = 5.64 \pm 0.01$ S corresponding to a molecular mass of 105 ± 1 kDa as estimated by the program DCDT$^+$ (version 1.16, John S. Philo). However, at 2.5 M NaCl (buffer T, 25 °C) ([scRPA] = 1.5 μM) a lower sedimentation coefficient of 5.05 ± 0.04 S was obtained, corresponding to a lower molecular mass of 62 ± 1 kDa. These results indicate that scRPA is a stable heterotrimer at all [NaCl] values less than or equal to 1.5 M, but that partial dissociation of the scRPA heterotrimer appears to occur at 2.5 M NaCl.

We also examined the effects of 5 mM $MgCl_2$ and 1 mM DTT on the scRPA assembly state using sedimentation velocity (data not shown). In the presence of 20 mM NaCl (buffer T, 25 °C), scRPA sedimented as a single species with weight average sedimentation coefficients of $\bar{S}_{20,w} = 5.63 \pm 0.01$ and 5.61 ± 0.02 S in the presence of 5 mM $MgCl_2$ or 1 mM DTT, respectively, corresponding to molecular masses of 105 ± 1 and 101 ± 2 kDa, close to the expected value of 114 kDa.

Occluded Site Size of scRPA on Poly(dT). Any characterization of the ssDNA binding properties of a nonspecific ssDNA binding protein such as scRPA should include a determination of the occluded site size (n) when bound to ssDNA. This is defined as the number of ssDNA nucleotides that are occluded by one protein and thus prevented from interacting with a second protein (*62*). As mentioned above,

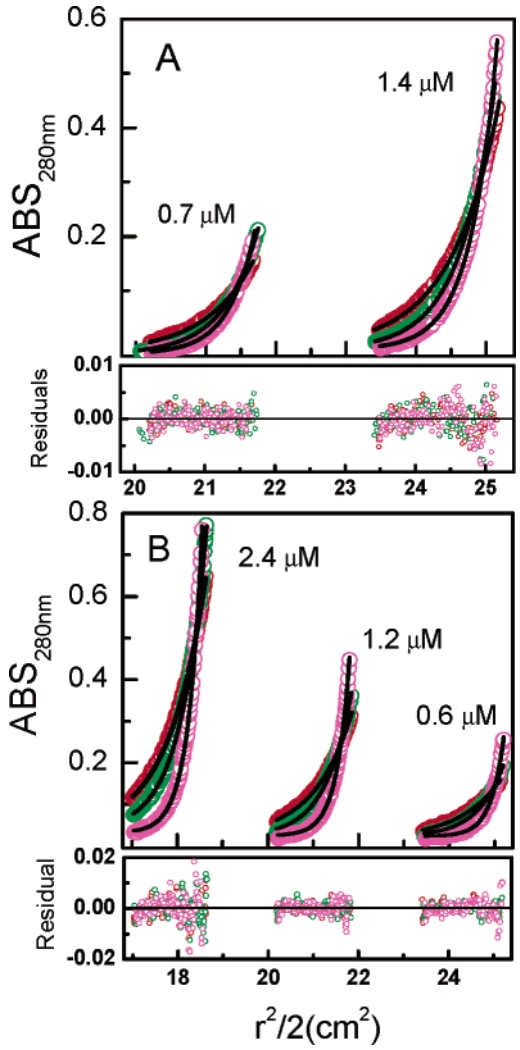

FIGURE 2: Stability of the scRPA heterotrimer as a function of [NaCl]. (A) Sedimentation equilibrium results at 20 mM NaCl (buffer T, 25 °C) for two scRPA concentrations (0.7 and 1.4 μM) and three rotor speeds of 10 krpm (red), 12 krpm (green), and 14 krpm (magenta). The solid curves represent the best global fits to a single-species model with a weight average molecular mass $M = 115 \pm 4.7$ kDa. (B) Sedimentation equilibrium results at 1.5 M NaCl (buffer T, 25 °C) for three scRPA concentrations (2.4, 1.2, and 0.6 μM) and three rotor speeds of 10 krpm (red), 14 krpm (olive), and 17 krpm (magenta). The solid curves represent the best global fits to a single-species model with a weight average molecular mass $M = 122 \pm 3.8$ kDa. The residuals for the fits are also shown below each data set.

although such estimates have been reported for scRPA, these estimates vary considerably, from 20 to 95 nucleotides (*29*, *48*, *49*). Such variation might result from differences due to the technique or approach used for the measurement, or it could reflect real differences that result from effects of the solution conditions. In fact, there is precedence for significant changes in the occluded site size for the *E. coli* SSB protein, a homotetrameric ssDNA binding protein, which can bind to ssDNA in multiple binding modes that differ in occluded site size, from ~33 ± 2 to 65 ± 3 nucleotides (*3*, *39*, *52*, *63*). These different binding modes are influenced by the salt concentration and type, including cation valence, pH, temperature, and protein binding density and reflect the fact that the *E. coli* SSB tetramer can bind to ssDNA using either all four or only two of its subunits, each of which contains an OB-fold, while still remaining tetrameric. In fact, it has

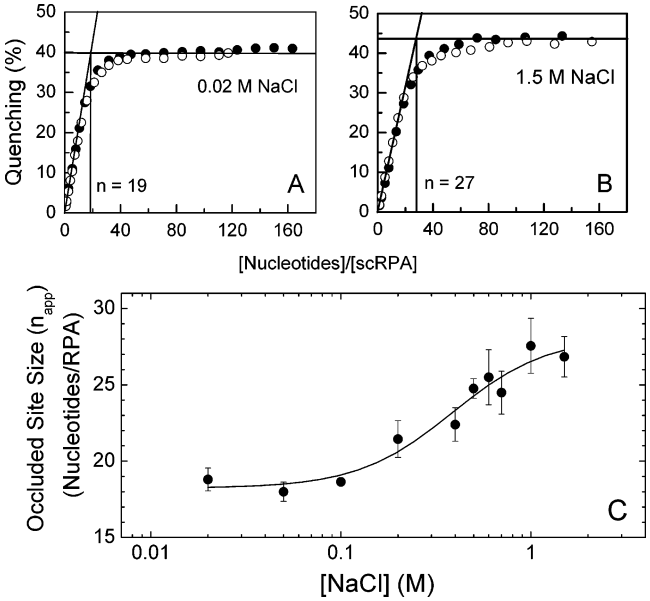

FIGURE 3: Salt dependence of the occluded site size for scRPA binding to poly(dT). Results of titrations of scRPA with poly(dT) (buffer T, pH 8.1, 25 °C) monitoring the quenching of scRPA tryptophan fluorescence (λ_{excit} = 295 nm and λ_{emis} = 345 nm) at (A) 20 mM NaCl and (B) 1.5 M NaCl. Each panel shows the results of two titrations obtained at two scRPA concentrations, (●) 0.1 μM and (○) 0.2 μM. The occluded site size (n_{app}) was determined from the intersection of the two lines as indicated and is 19 ± 1 nucleotides at 20 mM NaCl and 27 ± 2 nucleotides at 1.5 M NaCl. (C) n_{app} for scRPA binding to poly(dT) plotted as a function of [NaCl] (buffer T, pH 8.1, 25.0 °C). The solid line simulates the transition between a low salt binding mode with n = 18 ± 1 nucleotides and a high salt binding mode with n = 27 ± 2 nucleotides with a transition at ~0.36 M NaCl.

been hypothesized that RPA might also bind to ssDNA in multiple binding modes using different numbers of its OB-folds (*37*).

We therefore examined systematically the occluded site size for scRPA binding to the homopolynucleotide poly(dT) as a function of salt concentration to determine if a similar binding mode transition exists for scRPA. We first examined the effect of NaCl concentration (0.02−1.5 M) on the apparent occluded site size for scRPA binding to poly(dT). The scRPA protein has nine tryptophans (seven in RPA70, one in RPA32, and one in RPA14) (*64*)**,** and the intrinsic tryptophan fluorescence of scRPA is partially quenched upon binding ssDNA (*29*, *48*). We therefore used this tryptophan fluorescence quenching to monitor scRPA binding to poly(dT). Poly(dT) was used for several reasons. First, it remains single stranded and does not form intramolecular base pairs under a wide range of solution conditions. Second, scRPA binds with high affinity to poly(dT) (*48*), thus facilitating measurements of the occluded site size (*39*). The occluded site size measurements were performed by titrating scRPA with poly(dT) (see the Materials and Methods).

The results of two titrations performed at different NaCl concentrations (20 mM and 1.5 M) are shown in Figure 3. In each case, the Trp fluorescence quenching increases as a linear function of the poly(dT) concentration, eventually reaching a plateau of ~40−44% quenching at high poly(dT) concentrations. n is estimated from these plots as the ratio of the moles of poly(dT) nucleotides per mole of scRPA at the intersection of the straight lines defining the increase in Trp fluorescence quenching and the plateau. Titrations at each [NaCl] were performed at two or more scRPA concentrations (from 40 to 300 nM), and the apparent stoichiometries were found to be independent of scRPA concentration, indicating that binding is stoichiometric at each NaCl concentration.

Table 2: Occluded Site Size (n) of scRPA Binding to Poly(dT) under Different Buffer Conditions (10 mM Tris (pH 8.1), 0.1 mM Na_3EDTA, 25.0 °C)

[NaCl] (M)	[$MgCl_2$] (mM)	site size (nucleotide/scRPA)	[NaCl] (M)	[$MgCl_2$] (mM)	site size (nucleotide/scRPA)
0.02		19 ± 1	0.7		25 ± 1
0.05		18 ± 1	1.0		28 ± 2
0.1		19 ± 1	1.5		27 ± 2
0.2		21 ± 1		1.0	20 ± 1
0.4		22 ± 1		5.0	20 ± 1
0.5		25 ± 1		10.0	22 ± 1
0.6		26 ± 1			

Similar titrations were repeated at a series of [NaCl] values from 20 mM to 1.5 M, and the site sizes are plotted in Figure 3C. These data clearly show that the occluded site size (n_{app}) is affected by [NaCl]. A plateau value of n_{app} = 18−20 nucleotides is observed for [NaCl] ≤ 100 mM, but above 100 mM NaCl, n_{app} increases with increasing [NaCl], reaching a value of ~26−28 nucleotides at 1.0 and 1.5 M NaCl (see also Table 2). The maximum extent of Trp fluorescence quenching is relatively constant for the titrations performed at each [NaCl], although some variation in the final extent of fluorescence quenching (43−50%) is observed for measurements at 20 mM NaCl. This variation suggests that there may be some slow kinetic processes occurring, possibly reflecting slow protein−DNA rearrangements at 20 mM NaCl. Titrations at 2.0 M NaCl were also performed, but the binding affinity was not sufficiently high to allow an unambiguous determination of the site size. On the basis of the fact that scRPA undergoes partial disassembly at 2.5 M NaCl (see above), it seems likely that this may also occur at 2.0 M NaCl. In any event, these data show clear evidence for a [NaCl]-dependent change in occluded site size for scRPA binding to poly(dT). The midpoint of the transition occurs at approximately 0.36 M NaCl.

scRPA Binding to $(dT)_{30}$ ($L \geq n$) *Examined by Isothermal Titration Calorimetry*. If the change in occluded site size with increasing [NaCl] shown in Figure 3C reflects a change in the number of OB-folds that interact with the poly(dT), then this might also be detected as a change in the stoichiometry of scRPA binding to a ss oligodeoxythymidylate of length near the occluded site size. To test this, we examined the binding of scRPA to the oligodeoxythymidylate, $(dT)_{30}$, at high and low [NaCl]. Since the occluded site size is 18−20 nucleotides at low [NaCl] (0.02−0.2 M), but increases to 26−28 nucleotides at high [NaCl] (above 1.0 M), then $(dT)_{30}$ might bind only one scRPA molecule at high [NaCl], but two scRPA molecules at the lower [NaCl]. We examined this question using ITC, fluorescence titrations, and sedimentation equilibrium.

We first performed ITC titrations of scRPA with $(dT)_{30}$ at three [NaCl] (0.02, 0.2, and 1.5 M) (buffer T, pH 8.1, 25 °C), and the results are shown in Figure 4. The isotherm for scRPA binding to $(dT)_{30}$ obtained in 1.5 M NaCl (Figure 4A) is well described by a 1:1 binding model, yielding an equilibrium binding constant $K_{obsd} = (1.2 \pm 0.1) \times 10^8\ M^{-1}$

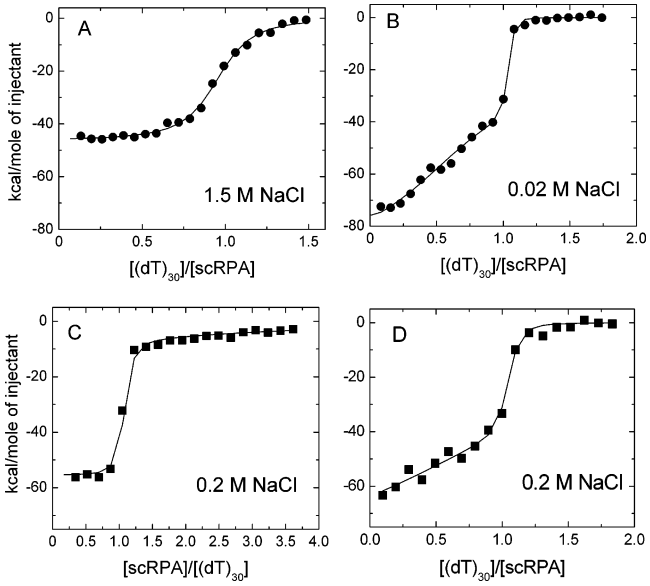

FIGURE 4: The stoichiometry of scRPA binding to $(dT)_{30}$ is influenced by [NaCl]. Results of ITC titrations of scRPA with $(dT)_{30}$, plotted as normalized heat per mole of injectant (panels A, B, and D) and of $(dT)_{30}$ with scRPA (panel C). (A) Titration of scRPA (0.72 μM) with $(dT)_{30}$ (6.4 μM) at 1.5 M NaCl (buffer T, pH 8.1, 25 °C). The solid line represents the best fit of the data to a single-site binding model (eq 7a), yielding $K = (1.21 \pm 0.14) \times 10^8$ M^{-1} and $\Delta H_{obsd} = -46.2 \pm 0.5$ kcal/mol. (B) Titration of scRPA (0.6 μM) with $(dT)_{30}$ (6.2 μM) at 20 mM NaCl (buffer T, pH 8.1, 25 °C). The solid line represents the best fit to a two-site binding model (eq 8a), yielding $K_1 = (1.6 \pm 0.8) \times 10^{10}$ M^{-1}, $\Delta H_1 = -56.5 \pm 0.5$ kcal/mol and $K_2 = (2.4 \pm 1.5) \times 10^6$ M^{-1}, $\Delta H_2 = -32.7 \pm 10.0$ kcal/mol. (C) Titration of $(dT)_{30}$ (0.43 μM) with scRPA (15.1 μM) at 0.20 M NaCl (buffer T, pH 8.1, 10% (v/v) glycerol, 25 °C). The solid line represents the best fit to a two-site binding model (eq 8a), yielding $K_1 = (9.3 \pm 5.6) \times 10^8$ M^{-1}, $\Delta H_1 = -55.4 \pm 1.1$ kcal/mol and $K_2 = (6.0 \pm 5.2) \times 10^5$ M^{-1}, $\Delta H_2 = -37.1 \pm 19.0$ kcal/mol. (D) Titration of scRPA (1.1 μM) with $(dT)_{30}$ (21.1 μM) performed in the same buffer conditions as in (C). The solid line represents the best fit to a two-site binding model (eq 8a), yielding $K_1 = (8.9 \pm 4.5) \times 10^8$ M^{-1}, $\Delta H_1 = -51.6 \pm 1.0$ kcal/mol and $K_2 = (5.3 \pm 5.5) \times 10^5$ M^{-1}, $\Delta H_2 = -30.2 \pm 22.0$ kcal/mol.

and a binding enthalpy $\Delta H_{obsd} = -46.2 \pm 0.5$ kcal/mol. However, at the lower salt concentration (20 mM NaCl) (Figure 4B), the shape of the binding isotherm is distinctly different. In addition, the binding enthalpy at excess scRPA (low values of $[(dT)_{30}]/[scRPA]$) is considerably more negative (~ -75 kcal/mol of $(dT)_{30}$) in 20 mM NaCl than in 1.5 M NaCl (~ -46 kcal/mol). The data in Figure 4B indicate that two scRPA heterotrimers are able to bind to a single $(dT)_{30}$ molecule. At low ratios of $[(dT)_{30}]_{tot}$ to $[scRPA]_{tot}$ a mixture of 1:1 and 2:1 complexes exists; however, only the 1:1 complex is observed at higher $[(dT)_{30}]_{tot}$. We note that the shape of the binding isotherm in Figure 4B indicates that the second scRPA molecule binds with lower apparent affinity than does the first one (apparent negative cooperativity), since saturation at $[(dT)_{30}]_{tot}/[scRPA]_{tot} = 0.5$ would be expected if binding of two scRPA molecules occurred with a large positive cooperativity. The titrations in Figure 4B can be fit to a model in which two scRPA molecules bind sequentially to $(dT)_{30}$ (see the Materials and Methods), yielding $K_{1,obsd} = (1.6 \pm 0.8) \times 10^{10}$ M^{-1}, $\Delta H_1 = -56.5 \pm 0.5$ kcal/mol and $K_{2,obsd} = (2.4 \pm 1.5) \times 10^6$ M^{-1}, $\Delta H_2 = -32 \pm 10$ kcal/mol.

The ability of $(dT)_{30}$ to bind two scRPA molecules is also apparent from titrations performed in 0.20 M NaCl (buffer T, pH 8.1, 10% (v/v) glycerol), where the estimated occluded site size on poly(dT) is low ($n_{app} = 21-22$ nucleotides; see Table 2). In this case, we performed titrations in both the "forward" (titrating scRPA in the cell with $(dT)_{30}$ (Figure 4C)) and "reverse" (titrating $(dT)_{30}$ in the cell with scRPA (Figure 4D) directions. The isotherm in Figure 4C indicates that a second molecule of RPA binds to $(dT)_{30}$ at $[RPA]_{tot}/[(dT)_{30}]_{tot} > 1$, although with lower macroscopic affinity, as judged by the gradual increase at $[RPA]_{tot}/[(dT)_{30}]_{tot} \gg 1$. The data in Figure 4C can be fit to a model for the sequential binding of two scRPA molecules (see the Materials and Methods), yielding $K_{1,obsd} = (9.3 \pm 5.6) \times 10^8$ M^{-1}, $\Delta H_1 = -55.4 \pm 1.1$ kcal/mol and $K_{2,obsd} = (6.0 \pm 5.2) \times 10^5$ M^{-1}, $\Delta H_2 = -37 \pm 19$ kcal/mol. The isotherm obtained from the "reverse" titration shown in Figure 4D can also be fit to the same model, yielding similar parameters, $K_{1,obsd} = (8.9 \pm 4.5) \times 10^8$ M^{-1}, $\Delta H_1 = -51.6 \pm 1.2$ kcal/mol and $K_{2,obsd} = (5.3 \pm 5.5) \times 10^5$ M^{-1}, $\Delta H_2 = -30 \pm 22$ kcal/mol. The large uncertainties in the estimates for $K_{2,obsd}$ and ΔH_2 are due to the low affinity and high correlation between these parameters. On the other hand, the estimate of ΔH_1 (-52 to -55 kcal/mol) is more reliable due to the higher apparent affinity for the binding of the first scRPA molecule. These results indicate that the binding of the second scRPA molecule to $(dT)_{30}$ occurs with an apparent binding constant that is $\sim 10^3$-fold lower than for the binding of the first molecule of scRPA. However, much of this apparent lower affinity is likely due to the nonspecific nature of the binding interaction; there are many more sites available on the DNA for binding of the first scRPA molecule ($30 - n + 1 = 13$ for the $n = 18$ mode of binding) than the single site available for the second scRPA molecule.

In general, these results are consistent with the effects of [NaCl] on the apparent site size for scRPA binding to poly(dT). Only one scRPA can bind to $(dT)_{30}$ at 1.5 M NaCl, where the occluded site size on poly(dT) is 26−28 nucleotides. However, at the lower [NaCl] (20 and 200 mM), where the occluded site size is only 18−20 nucleotides, two molecules of scRPA can bind to $(dT)_{30}$. These differences in site sizes and binding stoichiometries likely reflect the manifestation of alternative binding modes differing in the number of OB-folds that interact with the ssDNA.

Sedimentation Equilibrium Studies of scRPA Binding to (dT)$_{30}$. To further examine the stoichiometries of scRPA−$(dT)_{30}$ complexes we performed sedimentation equilibrium experiments. For these studies we used $(dT)_{29}$ labeled covalently with Cy3 at its 5′ end (Cy3-$(dT)_{29}$). Since the Cy3 moiety has an absorbance peak at 550 nm, this enabled us to monitor the sedimentation profile of Cy3-$(dT)_{29}$ without interference from the scRPA. Complex formation between Cy3-$(dT)_{29}$ and scRPA is detectable as an increase in the weight average molecular mass (M_{app}) of Cy3-$(dT)_{29}$; hence, such experiments should readily differentiate ssDNA bound with one or two scRPA molecules. These studies were performed in buffer T (pH 8.1, 25 °C) in the presence of either 20 mM NaCl or 1.5 M NaCl and at two molar ratios of $[scRPA]_{tot}$ to $[Cy3\text{-}(dT)_{29}]_{tot}$, one at a 4-fold excess of scRPA and the other at a 1:1 molar ratio.

The sedimentation equilibrium profiles at 20 mM NaCl are shown in Figure 5A,B for the experiments performed at

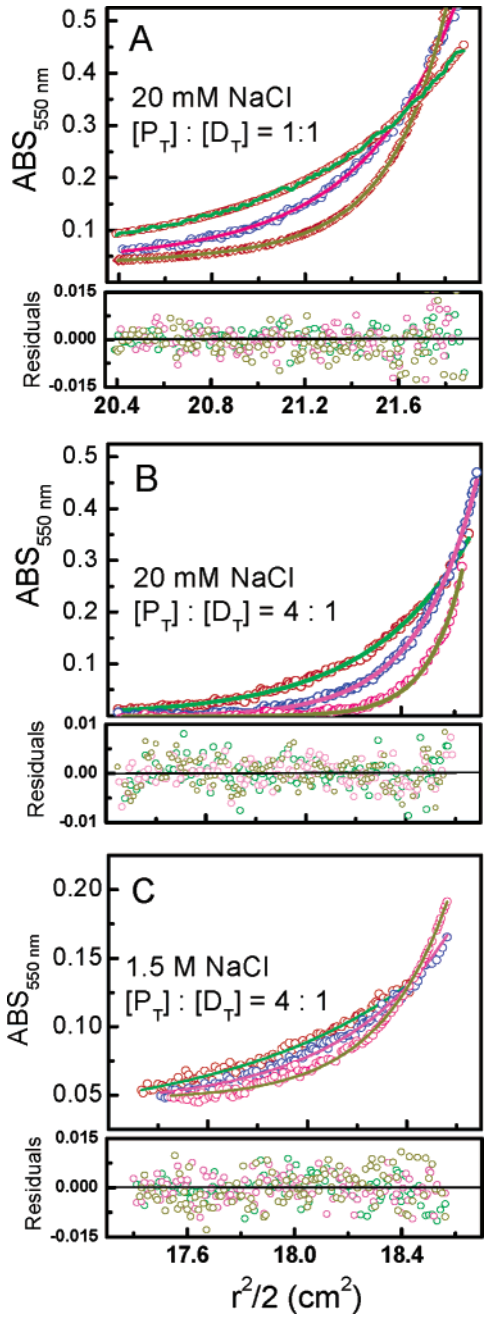

FIGURE 5: Stoichiometries of scRPA−5′-Cy3-$(dT)_{29}$ complexes examined by sedimentation equilibrium. (A) Results of experiments performed at a 1:1 molar ratio of scRPA (1.27 μM) to 5′-Cy3-$(dT)_{29}$ (1.27 μM) at 20 mM NaCl (buffer T, pH 8.1, 25 °C) at three rotor speeds, 10 krpm (green), 13 krpm (magenta), and 17 krpm (dark yellow). These data fit well to a single-species model (eq 1), yielding a molecular mass $M = 113 \pm 1$ kDa, which is close to that expected for a 1:1 complex (123 kDa). (B) Results of experiments performed at a 4-fold molar excess of scRPA (2.4 μM) over 5′-Cy3-$(dT)_{29}$ (0.6 μM) at 20 mM NaCl (buffer T, pH 8.1, 25 °C) at three rotor speeds, 10 krpm (green), 13 krpm (magenta), and 17 krpm (dark yellow). The data fit well to a single-species model (eq 1), yielding a weight average molecular mass $M = 222.8 \pm 2.0$ kDa, close to the expected value of 218 kDa for a complex of two scRPA molecules bound to one 5′-Cy3-$(dT)_{29}$ molecule. (C) Results of experiments performed at a 4-fold molar excess of scRPA (2.4 μM) over 5′-Cy3-$(dT)_{29}$ (0.6 μM) in 1.5 M NaCl (buffer T, pH 8.1, 25 °C) at three rotor speeds, 10 krpm (green), 13 krpm (magenta), and 17 krpm (dark yellow). The data fit well to a single-species model (eq 1), yielding a molecular mass $M = 127 \pm 3$ kDa, which is close to that expected for a 1:1 complex (123 kDa).

1:1 and 4:1 molar ratios of scRPA to ssDNA, respectively. Both sets of data are described well by a single-species model, as judged from the random distribution of residuals. The best nonlinear least-squares fit to the data at a 1:1 molar ratio yields a weight average molecular mass of 113.6 ± 1.0 kDa, whereas the best fit to the data at a 4:1 molar ratio yields a weight average molecular mass of 222.8 ± 2.0 kDa. The masses expected for Cy3-$(dT)_{29}$ bound with one or two scRPA molecules are 123 and 218 kDa, respectively. Hence, these results are consistent with the ITC experiments performed at the same NaCl concentration (20 mM) and indicate that a 1:1 complex can form at low [scRPA], but that a 2:1 complex can form at higher scRPA concentrations. On the other hand, sedimentation equilibrium experiments performed at 1.5 M NaCl indicate that only one scRPA can bind to the Cy3-$(dT)_{29}$ even at a 4:1 molar ratio (scRPA−5′-Cy3-$(dT)_{29}$) (see Figure 5C). The data in Figure 5C are well described by a single sedimenting species with a weight average molecular mass of 127.3 ± 2.9 kDa, consistent with a single scRPA bound per Cy3-$(dT)_{29}$.

We also determined the ability of scRPA to bind to $(dT)_{22}$ and $(dT)_{30}$ at low salt concentration (20 mM NaCl) in buffer T by using an electrophoretic mobility shift assay (EMSA) (data not shown). The experiments indicate that only 1:1 complexes are formed when both oligodeoxynucleotides are present in excess over scRPA. However, under conditions of excess protein, only one complex is formed with $(dT)_{22}$, whereas two bands are observed for scRPA binding to $(dT)_{30}$ at increasing ratios of $[scRPA]_{tot}$ to $[ssDNA]_{tot}$, indicating that both 1:1 and 2:1 complexes can form with $(dT)_{30}$ under low [NaCl] conditions.

Stoichiometry of scRPA Binding to Short ss Oligodeoxynucleotides ($L \leq n$) at 1.5 M NaCl Examined by Fluorescence Quenching. The occluded site sizes, $n = 18-20$ and $n = 26-28$, determined for scRPA binding to poly(dT) at low and high salt concentrations, respectively, suggest that a single scRPA protein could potentially bind more then one ss oligodeoxynucleotide if the length of the oligodeoxynucleotide, L, is less than n. To examine this, we investigated a series of $(dT)_L$ oligodeoxynucleotides with L varying from 16 to 28 nucleotides (i.e., with $L \leq n$). For these experiments we monitored $(dT)_L$ binding by the quenching of the scRPA Trp fluorescence. These experiments were performed at 1.5 M NaCl (buffer T, pH 8.1, 25 °C). Experiments were also performed at 20 mM NaCl; however, those titrations displayed large variations in fluorescence quenching amplitudes and thus were not suitable for quantitative analysis. The experiments performed at 1.5 M NaCl were well behaved.

The binding of scRPA to $(dT)_L$ (for $L = 28$, 26, 22, 20, 18, and 16 nucleotides) was examined in 1.5 M NaCl (buffer T, pH 8.1, 25 °C). Recall that n determined with poly(dT) is 26−28 nucleotides under these conditions (see Table 2). The results of scRPA titrations with $(dT)_{28}$ and $(dT)_{20}$ are shown in parts A and C, respectively, of Figure 6. In both cases, two or more titrations were performed at different scRPA concentrations and the titrations were analyzed using the model-independent binding density function analysis (*59*) to determine the relationship between the average fluorescence quenching signal and the average extent of $(dT)_L$ binding per scRPA. The results, plotted in Figure 6B (for $(dT)_{28}$) and Figure 6D (for $(dT)_{20}$), demonstrate that the

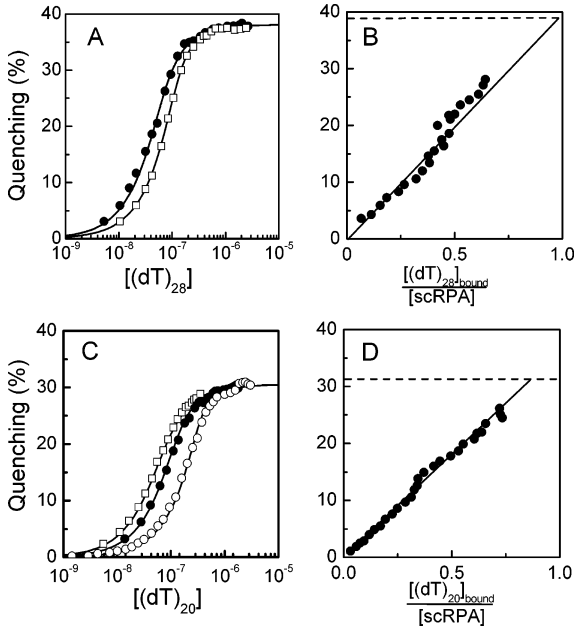

FIGURE 6: Fluorescence binding isotherms show that 1:1 complexes of scRPA with $(dT)_{28}$ and $(dT)_{20}$ are formed at 1.5 M NaCl. (A) Results of equilibrium fluorescence titrations of scRPA with $(dT)_{28}$ at two scRPA concentrations, (●) 6.0×10^{-8} M and (□) 1.2×10^{-7} M (buffer T, pH 8.1, 25 °C, 1.5 M NaCl), monitoring the quenching of the scRPA tryptophan fluorescence. Global fitting of the two titrations to a single-site binding model (eq 5a) yields $K_{obsd} = (6.72 \pm 0.42) \times 10^7$ M^{-1} and $Q_{max} = 0.38 \pm 0.01$. The solid lines are simulations based on eq 5a and the best fit parameters. (B) Analysis of the data in panel A using the model-independent binding density function method shows that the fluorescence quenching of scRPA is directly proportional to the average number of $(dT)_{28}$ molecules bound per scRPA heterotrimer. Linear extrapolation of the data to the known maximum fluorescence quenching at saturation yields a stoichiometry of 1.0 $(dT)_{28}$/scRPA. (C) Results of equilibrium fluorescence titrations of scRPA with $(dT)_{20}$ at three scRPA concentrations, (□) 0.5×10^{-7} M, (●) 1.0×10^{-7} M, and (○) 3.0×10^{-7} M (buffer T, pH 8.1, 25 °C, 1.5 M NaCl). Global fitting of the two titrations to a single-site binding model (eq 5a) yields $K_{obsd} = (4.02 \pm 0.21) \times 10^7$ M^{-1} and $Q_{max} = 0.31 \pm 0.01$. The solid lines are simulations based on eq 5a and the best fit parameters. (D) Dependence of scRPA fluorescence quenching on the average number of $(dT)_{20}$ molecules bound per scRPA molecule, obtained from analysis of the data in panel C using the binding density function method. The solid line shows a linear extrapolation of the data to the known maximum fluorescence quenching at saturation yields a stoichiometry of 1.0 $(dT)_{20}$/scRPA.

average quenching increases linearly with the average extent of binding. Furthermore, a linear extrapolation to the maximum fluorescence quenching observed at saturation (Q_{max}) (plateau values in Figure 6A,C) indicates a 1:1 stoichiometry of binding. The isotherms are well described by a one-site binding model (see the Materials and Methods), as are all of the isotherms for $(dT)_L$ with $L = 20-28$ nucleotides. Nonlinear least-squares analysis of these binding isotherms yields the observed equilibrium binding constant (K_{obsd}) and Q_{max}, which are listed in Table 3 for $(dT)_L$, with $L = 20$, 22, 26, and 28 nucleotides. K_{obsd} decreases slightly (from $(6.7 \pm 0.4) \times 10^7$ to $(4.0 \pm 0.4) \times 10^7$ M^{-1}), as does Q_{max} (from 0.38 ± 0.01 to 0.30 ± 0.01), as L decreases from 28 to 20 nucleotides. This behavior is expected since the shorter oligodeoxythymidylates interact with fewer residues within the protein binding site.

We next examined the binding of scRPA to $(dT)_L$ with $L = 16$ and 18 nucleotides. For these shorter oligodeoxynucleotides, we detect binding of a second ssDNA molecule to scRPA. Titrations of scRPA with $(dT)_{18}$ at two scRPA concentrations (0.10 and 0.36 μM) in 1.5 M NaCl (buffer T, pH 8.1, 25 °C) are shown in Figure 7A. These titrations show clear biphasic behavior, indicating that more than one $(dT)_{18}$ molecule can bind to scRPA. Analysis of these titrations using the model-independent binding density function analysis (*59*) confirms a 2:1 binding stoichiometry (see Figure 7B). Binding of the first $(dT)_{18}$ molecule results in a fluorescence quenching of $Q_1 \approx 0.20$, while binding of two

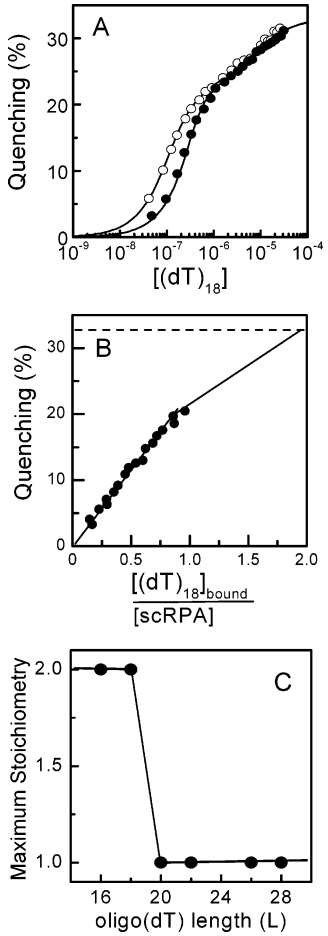

FIGURE 7: Equilibrium binding isotherms show that two molecules of $(dT)_{18}$ can bind per scRPA molecule at high salt concentration. (A) Equilibrium titrations monitoring the scRPA tryptophan fluorescence quenching upon binding $(dT)_{18}$ obtained at two scRPA concentrations, (○) 1.0×10^{-7} M and (●) 3.6×10^{-7} M, at 1.5 M NaCl (buffer T, pH 8.1, 25 °C). The continuous lines represent simulations based on a model for two molecules of $(dT)_{18}$ binding per scRPA molecule (eq 6a). A global NLLS fit of both titrations yields $K_{1,obsd} = (2.08 \pm 0.22) \times 10^7$ M^{-1} and $K_{2,obsd} = (1.29 \pm 0.26) \times 10^5$ M^{-1} for the macroscopic binding constants for binding of the first and the second $(dT)_{18}$ molecules to scRPA. (B) Dependence of the relative tryptophan fluorescence quenching of scRPA on the average number of $(dT)_{18}$ molecules bound per scRPA molecule obtained from analysis of the titrations in panel A. The relationship for the second phase of the titrations could not be obtained due to the weak binding affinity. However, a linear extrapolation from the points at $[(dT)_{18}]/[scRPA] = 1$ to the known maximum fluorescence quenching at saturation ($Q_{max} = 0.33 \pm 0.01$) yields a maximum stoichiometrry of 2 mol of $(dT)_{18}$ bound per mole of scRPA. (C) Dependence of the maximum stoichiometry (maximum number of $(dT)_L$ molecules that can bind per scRPA molecule) as a function of the ss oligodeoxythymidylate length, L (1.5 NaCl, buffer T, pH 8.1, 25 °C), showing a clear transition between $L = 18$ and $L = 20$ nucleotides.

Table 3: Thermodynamic and Spectroscopic Properties for the Binding of ssDNA Oligomers to scRPA in Buffer T, 1.5 M NaCl, at 25 °C

$(dT)_L$ length	absolute stoichiometry	$K_{1,obsd} \times 10^{-7}$ (M^{-1})	$K_{2,obsd} \times 10^{-5}$ (M^{-1})	Q_1	Q_2	Q_{max}
18	2	2.1 ± 0.2	1.3 ± 0.3	0.23 ± 0.01	0.10 ± 0.01	0.33 ± 0.01
20	1	4.0 ± 0.2				0.31 ± 0.01
22	1	2.7 ± 0.2				0.32 ± 0.01
26	1	5.0 ± 0.2				0.33 ± 0.01
28	1	6.7 ± 0.4				0.38 ± 0.01

$(dT)_{18}$ molecules results in a total quenching of $Q_{max} \approx 0.33$. The data in Figure 7A can be globally fit to a two-site binding model (see the Materials and Methods), yielding macroscopic binding constants for the first $(dT)_{18}$ molecule, $K_{1,obsd} = (2.1 \pm 0.2) \times 10^7\ M^{-1}$, and for the second $(dT)_{18}$ molecule, $K_{2,obsd} = (1.3 \pm 0.5) \times 10^5\ M^{-1}$, with corresponding values of quenching, $Q_1 = 0.23 \pm 0.01$ and $Q_2 = 0.10 \pm 0.01$ (see Table 3). Similar experiments performed with $(dT)_{16}$ also show that 2 mol of $(dT)_{16}$ can bind per mole of scRPA at saturation (data not shown).

The maximum stoichiometries for the binding of $(dT)_L$ as a function of L are plotted in Figure 7C. Clearly, for the binding of $(dT)_{16}$ or $(dT)_{18}$, there is sufficient room remaining within the scRPA binding site to form a stable interaction with at least part of a second oligodeoxynucleotide. In the case of $(dT)_{16}$ there may be as many as 12 nucleotides of the second $(dT)_{16}$ molecule that can interact with scRPA. However, for $L \geq 20$ nucleotides, only 1:1 complexes are observed.

Estimation of the scRPA Contact Size by Isothermal Titration Calorimetry. n provides a measure of the number of nucleotides that are occluded by one scRPA molecule upon binding to poly(dT), such that a second scRPA molecule is unable to access these nucleotides. The contact size, m, is defined as the number of contiguous nucleotides required to form all interactions with the protein; hence, $m \leq n$. To estimate the contact size for scRPA binding to ssDNA, we performed ITC titrations of scRPA with a series of $(dT)_L$ oligodeoxynucleotides at 1.5 M NaCl (buffer T, pH 8.1) to determine how the equilibrium binding constant, K_{obsd}, and the binding enthalpy, ΔH_{obsd}, are affected by L. The magnitude of ΔH_{obsd} is expected to increase as the number of nucleotides involved in interactions with the protein increases until m is reached.

Figure 8A shows representative data from an ITC experiment in which $(dT)_{28}$ was titrated into a solution of scRPA (0.24 μM) in 1.5 M NaCl (buffer T, 25 C). These data are replotted as the injection heats normalized to the amount of injected DNA in Figure 8B. The smooth curve in Figure 8B represents the best fit of these data to a 1:1 binding isotherm (eq 7a), with equilibrium constant $K_{obsd} = (4.8 \pm 0.5) \times 10^7\ M^{-1}$ and $\Delta H_{obsd} = -47.1 \pm 0.9$ kcal/mol. A series of such experiments were performed as a function of the oligodeoxynucleotide length, for $L = 16-34$ nucleotides, and the ΔH_{obsd} values for binding of a single $(dT)_L$ are plotted as a function of L in Figure 8C. These results show that ΔH_{obsd} decreases (becoming more negative) with a fairly linear dependence on L up to $L = 28$ nucleotides and then levels off at $\Delta H_{obsd} = -46 \pm 1$ kcal/mol. m estimated from these data is ~28 nucleotides, which is equal to the occluded site size measured with poly(dT) under the same conditions.

Analysis of the ITC binding isotherms also yields the macroscopic equilibrium binding constants, $K_{obsd,L}$, which are plotted as a function of L in Figure 8D. Two phases are observed in this plot. The values of $K_{obsd,L}$ increase only slightly (by a factor of ~4) as L increases from 16 to 28 nucleotides and then increase more substantially as L increases from 28 to 34 nucleotides. The phase in the range $L < m$ results from the fact that, as L decreases, fewer contacts are made with the protein. The dependence of $K_{obsd,L}$ on L in this region will depend on the nature of the ssDNA binding site within scRPA. The dependence of $K_{obsd,L}$ on L in the range $L > m$ can be explained by the fact that scRPA is a nonspecific DNA binding protein, and thus, the number of available binding sites for scRPA on $(dT)_L$ will increase as L increases and is expected to follow eq 9 (*62*, *65*)

$$K_{obsd,L} = K_{int}(L - m + 1) \qquad (9)$$

where the intrinsic binding constant K_{int} is the binding constant for scRPA binding to an oligodeoxynucleotide with $L = m$). If we use eq 9 to describe the linear dependence of $K_{obsd,L}$ on L from $L = 28$ to $L = 34$ nucleotides in Figure

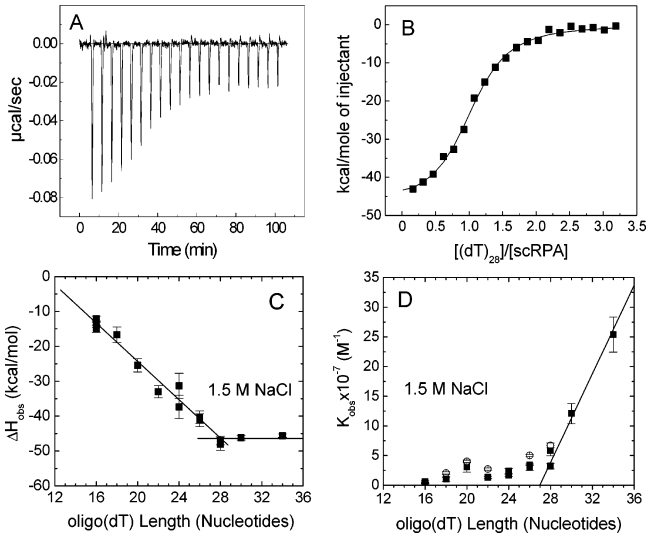

FIGURE 8: Determination of the scRPA contact size at 1.5 M NaCl. (A) Results of an ITC titration of scRPA (0.24 μM in the cell) with $(dT)_{28}$ (5.0 μM in the syringe) (buffer T, pH 8.1, 1.5 M NaCl, 25 °C). (B) Integrated heat responses from the data in (A) are plotted as injection heats (kcal) per mole of injected DNA. The smooth line represents the best fit to a 1:1 binding model (eq 7a) with parameters $K_{obsd} = (4.8 \pm 0.5) \times 10^7$ and $\Delta H_{obsd} = -47 \pm 1$ kcal/mol. (C) Dependence of ΔH_{obsd} on the ssDNA length, L, determined for scRPA binding to a series of oligodeoxynucleotides, $(dT)_L$ (buffer T, pH 8.1, 1.5 M NaCl, 25 °C). A contact size of $m = 28$ nucleotides is estimated from the intercept of the line describing the linear dependence of ΔH_{obsd} on L, with a plateau value of $\Delta H_{obsd} = -46 \pm 2$ kcal/mol at $L \geq 30$. (D) Dependence of the observed equilibrium binding constant, K_{obsd}, on the ss oligodeoxynucleotide length, L: (■) data from ITC titrations, (○) data from fluorescence titrations. A contact size of $m = 27-28$ nucleotides is determined from the intercept of a linear extrapolation of the data for $L \geq 28$ nucleotides to $K_{obsd} = 0$.

8D, we estimate $m = \sim 28$ nucleotides, which is consistent with the estimate obtained from analysis of the data in Figure 8C. Both estimates of m are the same within our uncertainties as the estimate of n for scRPA binding at 1.5 M NaCl.

Effects of Salt Concentration on the scRPA−$(dT)_{26}$ Binding Affinity. To obtain information about the electrostatic aspects of scRPA binding to ssDNA, we examined the effects of the monovalent salts NaCl and NaBr on the equilibrium constant, K_{obsd}, for scRPA binding to $(dT)_{26}$. We chose to examine $(dT)_{26}$ since the occluded site size of scRPA is ∼26−28 nucleotides at high [NaCl] (1.5 M). Binding was monitored by the quenching of the scRPA tryptophan fluorescence upon titration with $(dT)_{26}$ (buffer T, pH 8.1, 0.1 mM EDTA, 25.0 °C). The results of titrations performed as a function of [NaCl] and [NaBr] are shown in parts A and B, respectively, of Figure 9. At each salt concentration, the binding isotherms are well described by a simple 1:1 binding model. For each salt type, as the salt concentration is increased, the binding isotherms are shifted toward higher $(dT)_{26}$ concentrations, indicating that the binding constant decreases with increasing salt concentrations. In addition, the maximum fluorescence quenching accompanying saturation of scRPA with $(dT)_{26}$ decreases with increasing salt concentration. The dependences of K_{obsd} on [NaCl] and [NaBr] (log−log plots) are shown in Figure 9C. Both plots are linear over the salt concentration ranges examined, with slopes of $(\partial \log K)/(\partial \log [NaCl]) = -3.42 \pm 0.07$ and $(\partial \log K)/(\partial \log [NaBr]) = -3.87 \pm 0.15$, indicating that the binding of $(dT)_{26}$ is accompanied by a net release of 3−4 ions (cations and/or anions). Clearly, there is an effect of anion type in that the binding affinity is higher in the presence of Cl^- than in the presence of Br^-. Such effects have also been observed for the *E. coli* SSB protein binding to ssDNA (*60*, *66*, *67*).

The Cooperativity of scRPA Binding to M13ssDNA Is Low. Single-stranded binding proteins are commonly thought to bind cooperatively to long ssDNA and thus be capable of forming clusters of protein on ssDNA. This view stems primarily from the fact that the first SSB protein that was identified, the phage T4 gene 32 protein, shows highly cooperative binding to ssDNA (*1*, *53*). In addition, the *E. coli* SSB tetramer shows highly cooperative binding in its $(SSB)_{35}$ binding mode, although binding is not very cooperative in its fully wrapped $(SSB)_{65}$ binding mode (*41*, *61*, *66*). Studies examining the cooperativity of scRPA binding to ssDNA have been reported, although the conclusions have differed significantly. It was shown that both scRPA and hsRPA bind to ssDNA with low cooperativity (nearest neighbor cooperativity parameter $\omega = 10-20$) (*48*, *68*) using both fluorescence quenching and electrophoretic mobility shift assays (EMSA). However, using fluorescence quenching, Alani et al. (*29*) reported that binding of scRPA is highly cooperative, with $\omega = 10^4$ to 10^5. Since the different *E. coli* SSB binding modes display very different cooperativities for ssDNA binding, we wished to determine whether the two scRPA binding modes that we observe might also display different cooperativities.

The binding affinity of scRPA for poly(dT) is too high (stoichiometric binding) under all of the solution conditions examined here, and thus, we cannot obtain a quantitative estimate of the cooperativity for scRPA binding to poly(dT) under these conditions. To examine this issue qualitatively,

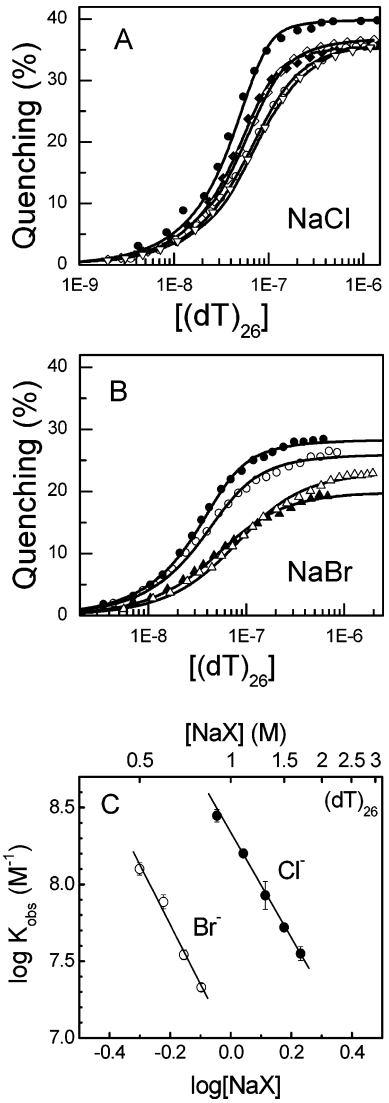

FIGURE 9: Dependence on NaCl and NaBr concentrations of the equilibrium constant for scRPA binding to $(dT)_{26}$. Equilibrium binding was monitored by the quenching of scRPA (50−90 nM) tryptophan fluorescence upon binding $(dT)_{26}$ (buffer T, pH 8.1, 25 °C). (A) Binding isotherms obtained as a function of [NaCl]: 0.90 M (●), 1.10 M (◆), 1.30 M (◇), 1.50 M (○), and 1.70 M (▽). Solid lines represent best fits of the data to a single-site binding model (eq 5a). (B) Binding isotherms obtained as a function of [NaBr]: 0.50 M (●), 0.60 M (○), 0.70 M (△), and 0.80 M (▲). Solid lines represent best fits of the data to a single-site binding model (eq 5a). (C) Dependence of K_{obsd} (obtained from analysis of the data in panels A and B) on the salt concentration (log−log plots), $(\partial \log K)/(\partial \log [NaCl]) = -3.42 \pm 0.07$ and $(\partial \log K)/(\partial \log [NaBr]) = -3.87 \pm 0.15$.

we used an agarose gel electrophoresis assay described previously for examination of the cooperativity of *E. coli* SSB binding to single-stranded DNA in its different binding modes (*61*). We examined the binding cooperativity of scRPA to circular M13mp18 ssDNA from bacteriophage M13 at two different [NaCl] (20 mM and 1.5 M) (see the Materials and Methods). Complexes of scRPA with ssM13mp18 DNA were formed at varying scRPA to DNA ratios by directly mixing the scRPA and DNA in defined solution conditions (buffer T, 22 °C) at a given [NaCl] and allowed to equilibrate for 1 h before electrophoresis. The gels were run in a low salt buffer (pH 7.8, 20 mM Tris,

0.4 mM sodium acetate, 0.2 mM Na_3EDTA) to minimize redistribution of scRPA molecules during electrophoresis. The scRPA−ssM13 DNA complexes were then electrophoresed in a 0.5% agarose gel, which separates the DNA molecules according to the amount of scRPA bound to each DNA molecule; the free ssDNA migrates fastest, and DNA with increasing amount of bound SSB migrates progressively slowest.

In this type of experiment, a protein that binds with very high cooperativity to DNA would yield a bimodal distribution of DNA molecules, consisting of two sharp bands representing DNA that was fully saturated with the protein and totally free DNA in the limit of a large excess of nucleic acid (low binding density). A noncooperatively binding protein, on the other hand, is expected to be distributed randomly among the ssDNA molecules, and hence, a single, more diffuse band should be observed at all binding densities. For the experiment performed at 20 mM NaCl, where the occluded site size is 18−20 nucleotides, the gel patterns show a broad binding density distribution and a single, somewhat diffuse band at each scRPA concentration, indicating low cooperativity (see Figure 1SA in the Supporting Information). The identical experiments performed at 1.5 M NaCl, where the occluded site size is ∼28 nucleotides, also show a single, diffuse band at low ratios of scRPA to DNA (see Figure 1SB in the Supporting Information). We note that the fluorescence titration experiments of Alani et al. (*29*) that were used to conclude that scRPA binds with high cooperativity to ssDNA were performed in the presence of high $MgCl_2$ concentrations (140−160 mM). We therefore also examined scRPA binding to ssDNA under these conditions using the agarose gel electrophoresis assay, but observed low cooperativity behavior similar to that observed in the absence of $MgCl_2$. Therefore, we find that scRPA binding to ssDNA under these conditions does not exhibit highly cooperative binding to ssDNA, which is consistent with reports that the cooperativity of scRPA binding to ssDNA is only low or moderate (*48*).

DISCUSSION

The eukaryotic RPA protein plays a central role in DNA metabolism (*5*). The heterotrimeric protein contains six OB-folds (see Figure 1) and thus six potential ssDNA binding domains. On the basis of this, there has been speculation concerning whether all or only a subset of these OB-folds interact with ssDNA and whether RPA might use different subsets of these OB-folds to bind ssDNA in alternate "binding modes". In fact, such multiple binding modes have been observed for the homotetrameric *E. coli* SSB protein, which contains four OB-folds (one per subunit). At least two of the *E. coli* SSB binding modes differ by the number of subunits that interact with the ssDNA (*3*, *4*). The binding properties of the different *E. coli* SSB binding modes differ substantially, including both site size and intertetramer cooperativity (*3*). Philipova et al. (*37*) first recognized that RPA contains at least four OB-folds and by analogy with the *E. coli* SSB protein suggested that RPA may also bind to ssDNA using multiple binding modes differing by the number of OB-folds used to contact the ssDNA.

On the basis of studies of oligodeoxynucleotide binding to hsRPA, it was proposed that hsRPA can bind to ssDNA in two binding modes, an unstable 8 nucleotide (nt) mode, observable only by cross-linking studies, and a larger stable 30 nt binding mode (*28*, *69*). Measurements of the ssDNA binding site size for RPA have been reported for a number of other organisms, although the reported values vary considerably, 22 nt's for *D. melanogaster* (*32*) and 20−25 nt's for calf (*30*), and the largest range of values has been reported for yeast, from 20−30 nt's (*49*) to 45 nt's (*48*) to 90 nt's (*29*). By systematically mutating each OB-fold, Bastin-Shanower (*27*) concluded that OB-folds A, B, and C interact with 12 nt's and that OB-fold D also interacts with ssDNA, but only when it is longer than 23 nt's. Recent reviews of the RPA structure suggest that OB-folds A and B interact with 8−10 nt's, OB-folds A, B, and C interact with 13−14 nt's, and all four OB-folds (A, B, C, and D) occlude 30 nt's. Others have concluded that two binding modes exist, the 8 nt unstable mode and the 30 nt stable mode (*50*). In addition to the confusion concerning the different reported site sizes and potential binding modes, no previous studies have provided evidence that RPA can bind to ssDNA in stable alternate binding modes or that RPA can undergo reversible transitions between alternate binding modes.

In the study reported here, we used four approaches and three techniques to examine the modes of scRPA binding to ssDNA. These experiments were performed with scRPA that was purified using a ssDNA cellulose column as the last purification step; hence, all of the scRPA was selected for ssDNA binding activity, and thus, it was not necessary to correct for the presence of inactive scRPA. The approaches used included direct measurements of the occluded site size on poly(dT) by monitoring the number of nucleotides needed to saturate the scRPA tryptophan fluorescence quenching. We also examined the equilibrium binding of scRPA to a series of ss oligodeoxythymidylates, $(dT)_L$, using sedimentation equilibrium, ITC, and fluorescence to measure both the equilibrium binding constant and ΔH_{obsd} of binding as a function of L. Each of these sets of experiments indicates that scRPA can undergo a salt-dependent transition between two stable ssDNA binding modes in vitro.

One binding mode has an occluded site size of 18−20 nucleotides and is favored at low salt concentration, while a second binding mode has a larger occluded site size of 26−28 nucleotides and is stabilized at [NaCl] > 500 mM. When combined with previous studies (*27*), it seems most likely that the low site size mode involves ssDNA interactions with OB-folds A, B, and C only within RPA70, while the higher site size mode involves those as well as additional interactions with OB-fold D within RPA32, as depicted in Figure 10. This is also consistent with the available structural information that a single OB-fold binds about four nucleotides, while an additional two nucleotides are needed to bridge the gap between two OB-folds (*21*, *70*). This structural information predicts that 16−17 nucleotides would be needed to bind three OB-folds in tandem (e.g., A, B, and C), consistent with the observed site size of 18−20 nucleotides at 20 mM NaCl. This simple analysis would then suggest that the number of nucleotides needed to bind contiguously to four OB-folds (A, B, C, and D) is ∼22−23. However, since the fourth OB-fold (D) is located in a different subunit (RPA32), the number of nucleotides needed to bridge the gap between the C and D OB-folds is expected to be more

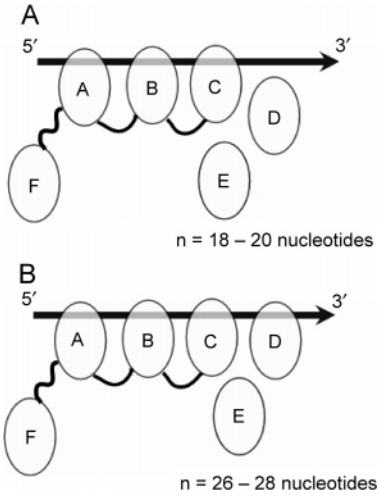

FIGURE 10: Schematic representation showing that the two scRPA modes of binding to long ssDNA differ in the number of OB-folds that interact with the ssDNA. (A) Low salt binding mode in which scRPA uses only three of its OB-folds (A, B, C) contained within the RPA70 subunit to bind ssDNA with an occluded site size of 18−20 nucleotides. (B) High salt binding mode in which scRPA uses the three OB-folds within the RPA70 subunit plus an additional OB-fold (D) from the RPA32 subunit to bind ssDNA with an occluded site size of 26−28 nucleotides.

than about two. Therefore, the larger site size of 26−28 nucleotides measured at 1.5 M NaCl is consistent with the involvement of OB-folds A, B, C, and D. Most RPA binding studies suggest that OB-fold E (RPA14) does not interact with ssDNA (*36*), while OB-fold F appears to be primarily involved in protein−protein interactions (*71*, *72*). However, we cannot rule out that OB-fold F also interacts with ssDNA in the higher site size binding mode.

We find no evidence for the putative eight nucleotide binding mode, consistent with it not being a stable binding mode. In fact, the previous studies simply indicated that an eight nucleotide long ssDNA could be cross-linked with glutaraldehyde to hsRPA (*28*). Such experiments cannot in general be used as a measure of a site size and also do not represent evidence for a distinct binding mode. Rather they simply indicate that a short oligodeoxynucleotide can be cross-linked to hsRPA.

The observation of a salt-dependent change in binding mode for scRPA has precedence in another SSB protein. The *E. coli* SSB homotetramer can bind to ssDNA in multiple binding modes differing in both occluded site size and cooperativity (*3*). However, the salt-dependent increase in the occluded site size observed for scRPA, from 18−20 nucleotides to 26−28 nucleotides, is not as dramatic as for the *E. coli* SSB protein (33−65 nucleotides) (*39*). Whereas the scRPA binding mode transition appears to involve a switch from a mode using three OB-folds to bind ssDNA to a mode using four OB-folds, the *E. coli* SSB protein undergoes a transition from a mode using two OB-folds to one using four OB-folds. However, in both cases, the presence of multiple OB-folds within the protein is the feature that allows for these binding mode transitions.

The molecular basis for the binding mode switch in scRPA, as well as any potential functional role for the two modes, is not known. In the case of *E. coli* SSB, two of the modes differ dramatically in their abilities to bind cooperatively to ssDNA (*41*, *61*). In addition, there is a salt-dependent negative cooperativity for ssDNA binding within the *E. coli* SSB tetramer (*67*, *73*, *74*). This results in a much lower affinity for ssDNA for binding to the second two subunits (OB-folds) within the tetramer. However, this negative cooperativity diminishes with increasing salt concentration, making it easier to bind ssDNA to all four subunits as the salt concentration increases, with a corresponding increase in site size when bound to long ssDNA. It remains to be seen whether a similar negative cooperativity exists within scRPA.

Previous studies of the cooperative binding of multiple RPA molecules to long ssDNA have also reported conflicting results. Most studies have concluded that RPA binds with little or moderate cooperativity (*25*, *26*, *30*, *32*). However, Alani et al. (*29*) reported a very high positive cooperativity ($\omega = 10^4$ to 10^5) for scRPA binding to ssDNA. In addition, Blackwell and Borowiec (*28*) concluded that hsRPA binds cooperatively in its eight nt "binding mode". We examined this issue qualitatively by agarose gel electrophoresis of scRPA−ssM13 phage complexes, which allowed us to observe the distribution of protein on the DNA, which has been used to identify proteins that bind with very high cooperativity to DNA (*61*). We always observed protein distributions on the ssDNA that indicated the absence of high cooperativity at both low and high [NaCl] (20 mM and 1.5 M), as well as in the presence of high concentrations of $MgCl_2$. Thus, at equilibrium, the scRPA protein does not appear to bind with very high cooperativity under our solution conditions in either binding mode. Our ITC and sedimentation equilibrium studies also support this conclusion and thus agree with the studies of Sibenaller et al. (*48*).

The results presented here demonstrate that scRPA can bind to long ssDNA in at least two binding modes in vitro and that the relative stability of these two modes is influenced by the salt concentration. Currently, there is no information available concerning which of these two modes, or whether possibly both, functions in vivo. However, in this context, it is also conceivable that other processes, such as posttranslational modifications of RPA subunits, or interactions with accessory proteins, could influence the relative stability of the RPA binding modes, since such modifications are known to modulate the role of RPA in DNA metabolism. For example, phosphorylation of RPA is believed to switch off DNA replication, but stimulate DNA repair processes (*75*, *76*). In fact, the RPA32 subunit, containing OB-fold D and the major sites for phosphorylation, does possess ssDNA binding activity (*27*, *77*, *78*), and recent studies have emphasized the role of RPA32 in many important processes such as DNA repair (*79*) and DNA replication (*77*). Therefore, it is possible that the higher site size binding mode reported here, which appears to be due to the additional interaction with ssDNA of the RPA32 OB-fold, may have a physiological role in DNA metabolism. It is also possible that phosphorylation of RPA32 may modulate both its DNA binding affinity and the relative stability of the different binding modes. Interestingly, recent studies show that a hyperphosphorylated form of hsRPA, in which five sites on the 70 kDa subunit and five sites on the 32 kDa subunit are phosphorylated, appears to have slightly reduced affinity for purine-rich ssDNA (*76*).

ACKNOWLEDGMENT

We thank Dr. Marc Wold for his generous gift of the scRPA expression vector and for very useful discussions with him and Dr. Peter Burgers. We thank T. Ho for synthesis and purification of the oligodeoxynucleotides used in this study and Dr. Anita Niedziela-Majka for assistance with the analytical ultracentrifugation experiments.

SUPPORTING INFORMATION AVAILABLE

Figure showing the results of agarose gel electrophoresis experiments at low (20 mM) and high (1.5 M) NaCl concentrations for scRPA−ssDNA complexes formed at different protein to DNA ratios, indicating low or no cooperativity upon formation of these complexes. This material is available free of charge via the Internet at http://pubs.acs.org.

REFERENCES

1. Alberts, B., Frey, L., and Delius, H. (1972) Isolation and characterization of gene 5 protein of filamentous bacterial viruses, *J. Mol. Biol. 68*, 139−152.
2. Kowalczykowski, S. C., Bear, D. G., and von Hippel, P. H. (1981) *Enzymes*, 3rd ed., Vol. XIV, pp 373−444.
3. Lohman, T. M., and Ferrari, M. E. (1994) Escherichia coli single-stranded DNA-binding protein: multiple DNA-binding modes and cooperativities, *Annu. Rev. Biochem. 63*, 527−570.
4. Raghunathan, S., Kozlov, A. G., Lohman, T. M., and Waksman, G. (2000) Structure of the DNA binding domain of E. coli SSB bound to ssDNA, *Nat. Struct. Biol. 7*, 648−652.
5. Wold, M. S. (1997) Replication protein A: a heterotrimeric, single-stranded DNA-binding protein required for eukaryotic DNA metabolism, *Annu. Rev. Biochem. 66*, 61−92.
6. Iftode, C., Daniely, Y., and Borowiec, J. A. (1999) Replication protein A (RPA): the eukaryotic SSB, *Crit. Rev. Biochem. Mol. Biol. 34*, 141−180.
7. Kenny, M. K., Lee, S. H., and Hurwitz, J. (1989) Multiple functions of human single-stranded-DNA binding protein in simian virus 40 DNA replication: single-strand stabilization and stimulation of DNA polymerases alpha and delta, *Proc. Natl. Acad. Sci. U.S.A. 86*, 9757−9761.
8. Brill, S. J., and Stillman, B. (1989) Yeast replication factor-A functions in the unwinding of the SV40 origin of DNA replication, *Nature 342*, 92−95.
9. Braun, K. A., Lao, Y., He, Z., Ingles, C. J., and Wold, M. S. (1997) Role of protein−protein interactions in the function of replication protein A (RPA): RPA modulates the activity of DNA polymerase alpha by multiple mechanisms, *Biochemistry 36*, 8443−8454.
10. Wakasugi, M., Shimizu, M., Morioka, H., Linn, S., Nikaido, O., and Matsunaga, T. (2001) Damaged DNA-binding protein DDB stimulates the excision of cyclobutane pyrimidine dimers in vitro in concert with XPA and replication protein A, *J. Biol. Chem. 276*, 15434−15440.
11. de Laat, W. L., Appeldoorn, E., Sugasawa, K., Weterings, E., Jaspers, N. G., and Hoeijmakers, J. H. (1998) DNA-binding polarity of human replication protein A positions nucleases in nucleotide excision repair, *Genes Dev. 12*, 2598−2609.
12. He, Z., Henricksen, L. A., Wold, M. S., and Ingles, C. J. (1995) RPA involvement in the damage-recognition and incision steps of nucleotide excision repair, *Nature 374*, 566−569.
13. Golub, E. I., Gupta, R. C., Haaf, T., Wold, M. S., and Radding, C. M. (1998) Interaction of human rad51 recombination protein with single-stranded DNA binding protein, RPA, *Nucleic Acids Res. 26*, 5388−5393.
14. Brosh, R. M., Jr., Li, J. L., Kenny, M. K., Karow, J. K., Cooper, M. P., Kureekattil, R. P., Hickson, I. D., and Bohr, V. A. (2000) Replication protein A physically interacts with the Bloom's syndrome protein and stimulates its helicase activity, *J. Biol. Chem. 275*, 23500−23508.
15. Brosh, R. M., Jr., Orren, D. K., Nehlin, J. O., Ravn, P. H., Kenny, M. K., Machwe, A., and Bohr, V. A. (1999) Functional and physical interaction between WRN helicase and human replication protein A, *J. Biol. Chem. 274*, 18341−18350.
16. Li, R., and Botchan, M. R. (1993) The acidic transcriptional activation domains of VP16 and p53 bind the cellular replication protein A and stimulate in vitro BPV-1 DNA replication, *Cell 73*, 1207−1221.
17. Cho, J. M., Song, D. J., Bergeron, J., Benlimame, N., Wold, M. S., and Alaoui-Jamali, M. A. (2000) RBT1, a novel transcriptional co-activator, binds the second subunit of replication protein A, *Nucleic Acids Res. 28*, 3478−3485.
18. Miller, S. D., Moses, K., Jayaraman, L., and Prives, C. (1997) Complex formation between p53 and replication protein A inhibits the sequence-specific DNA binding of p53 and is regulated by single-stranded DNA, *Mol. Cell. Biol. 17*, 2194−2201.
19. He, Z., Brinton, B. T., Greenblatt, J., Hassell, J. A., and Ingles, C. J. (1993) The transactivator proteins VP16 and GAL4 bind replication factor A, *Cell 73*, 1223−1232.
20. Murzin, A. G. (1993) OB(oligonucleotide/oligosaccharide binding)-fold: common structural and functional solution for non-homologous sequences, *EMBO J. 12*, 861−867.
21. Bochkarev, A., Pfuetzner, R. A., Edwards, A. M., and Frappier, L. (1997) Structure of the single-stranded-DNA-binding domain of replication protein A bound to DNA, *Nature 385*, 176−181.
22. Kerr, I. D., Wadsworth, R. I., Cubeddu, L., Blankenfeldt, W., Naismith, J. H., and White, M. F. (2003) Insights into ssDNA recognition by the OB fold from a structural and thermodynamic study of Sulfolobus SSB protein, *EMBO J. 22*, 2561−2570.
23. Brill, S. J., and Bastin-Shanower, S. (1998) Identification and characterization of the fourth single-stranded-DNA binding domain of replication protein A, *Mol. Cell. Biol. 18*, 7225−7234.
24. Arunkumar, A. I., Stauffer, M. E., Bochkareva, E., Bochkarev, A., and Chazin, W. J. (2003) Independent and coordinated functions of replication protein A tandem high affinity single-stranded DNA binding domains, *J. Biol. Chem. 278*, 41077−41082.
25. Kim, C., Paulus, B. F., and Wold, M. S. (1994) Interactions of human replication protein A with oligonucleotides, *Biochemistry 33*, 14197−14206.
26. Kim, C., Snyder, R. O., and Wold, M. S. (1992) Binding properties of replication protein A from human and yeast cells, *Mol. Cell. Biol. 12*, 3050−3059.
27. Bastin-Shanower, S. A., and Brill, S. J. (2001) Functional analysis of the four DNA binding domains of replication protein A. The role of RPA2 in ssDNA binding, *J. Biol. Chem. 276*, 36446−36453.
28. Blackwell, L. J., and Borowiec, J. A. (1994) Human replication protein A binds single-stranded DNA in two distinct complexes, *Mol. Cell. Biol. 14*, 3993−4001.
29. Alani, E., Thresher, R., Griffith, J. D., and Kolodner, R. D. (1992) Characterization of DNA-binding and strand-exchange stimulation properties of y-RPA, a yeast single-strand-DNA-binding protein, *J. Mol. Biol. 227*, 54−71.
30. Atrazhev, A., Zhang, S., and Grosse, F. (1992) Single-stranded DNA binding protein from calf thymus. Purification, properties, and stimulation of the homologous DNA-polymerase-alpha-primase complex, *Eur. J. Biochem. 210*, 855−865.
31. Brown, G. W., Melendy, T. E., and Ray, D. S. (1992) Conservation of structure and function of DNA replication protein A in the trypanosomatid Crithidia fasciculata, *Proc. Natl. Acad. Sci. U.S.A. 89*, 10227−10231.
32. Mitsis, P. G., Kowalczykowski, S. C., and Lehman, I. R. (1993) A single-stranded DNA binding protein from Drosophila melanogaster: characterization of the heterotrimeric protein and its interaction with single-stranded DNA, *Biochemistry 32*, 5257−5266.
33. Gomes, X. V., and Wold, M. S. (1996) Functional domains of the 70-kilodalton subunit of human replication protein A, *Biochemistry 35*, 10558−10568.
34. Walther, A. P., Gomes, X. V., Lao, Y., Lee, C. G., and Wold, M. S. (1999) Replication protein A interactions with DNA. 1. Functions of the DNA-binding and zinc-finger domains of the 70-kDa subunit, *Biochemistry 38*, 3963−3973.
35. Bochkarev, A., Bochkareva, E., Frappier, L., and Edwards, A. M. (1999) The crystal structure of the complex of replication protein A subunits RPA32 and RPA14 reveals a mechanism for single-stranded DNA binding, *EMBO J. 18*, 4498−4504.
36. Kolpashchikov, D. M., Weisshart, K., Nasheuer, H. P., Khodyreva, S. N., Fanning, E., Favre, A., and Lavrik, O. I. (1999) Interaction of the p70 subunit of RPA with a DNA template directs p32 to the 3′-end of nascent DNA, *FEBS Lett. 450*, 131−134.

37. Philipova, D., Mullen, J. R., Maniar, H. S., Lu, J., Gu, C., and Brill, S. J. (1996) A hierarchy of SSB protomers in replication protein A, *Genes Dev. 10*, 2222−2233.
38. Griffith, J. D., Harris, L. D., and Register, J., III (1984) Visualization of SSB-ssDNA complexes active in the assembly of stable RecA-DNA filaments, *Cold Spring Harbor Symp. Quant. Biol. 49*, 553−559.
39. Lohman, T. M., and Overman, L. B. (1985) Two binding modes in Escherichia coli single strand binding protein-single stranded DNA complexes. Modulation by NaCl concentration, *J. Biol. Chem. 260*, 3594−3603.
40. Lohman, T. M., and Bujalowski, W. (1990) Escherichia coli single strand binding protein: Multiple single-stranded DNA binding modes and cooperativities, in *The Biology of Nonspecific DNA-Protein Interactions* (Revzin, A., Ed.) pp 131−170, CRC Press, Boca Raton, FL.
41. Ferrari, M. E., Bujalowski, W., and Lohman, T. M. (1994) Cooperative binding of Escherichia coli SSB tetramers to single-stranded DNA in the (SSB)35 binding mode, *J. Mol. Biol. 236*, 106−123.
42. Lohman, T. M., and Bujalowski, W. (1994) Effects of base composition on the negative cooperativity and binding mode transitions of Escherichia coli SSB-single-stranded DNA complexes, *Biochemistry 33*, 6167−6176.
43. Bujalowski, W., Overman, L. B., and Lohman, T. M. (1988) Binding mode transitions of Escherichia coli single strand binding protein-single-stranded DNA complexes. Cation, anion, pH, and binding density effects, *J. Biol. Chem. 263*, 4629−4640.
44. Wei, T. F., Bujalowski, W., and Lohman, T. M. (1992) Cooperative binding of polyamines induces the Escherichia coli single-strand binding protein-DNA binding mode transitions, *Biochemistry 31*, 6166−6174.
45. Overman, L. B., and Lohman, T. M. (1994) Linkage of pH, anion and cation effects in protein-nucleic acid equilibria. Escherichia coli SSB protein-single stranded nucleic acid interactions, *J. Mol. Biol. 236*, 165−178.
46. Bochkareva, E., Belegu, V., Korolev, S., and Bochkarev, A. (2001) Structure of the major single-stranded DNA-binding domain of replication protein A suggests a dynamic mechanism for DNA binding, *EMBO J. 20*, 612−618.
47. Seroussi, E., and Lavi, S. (1993) Replication protein A is the major single-stranded DNA binding protein detected in mammalian cell extracts by gel retardation assays and UV cross-linking of long and short single-stranded DNA molecules, *J. Biol. Chem. 268*, 7147−7154.
48. Sibenaller, Z. A., Sorensen, B. R., and Wold, M. S. (1998) The 32- and 14-kilodalton subunits of replication protein A are responsible for species-specific interactions with single-stranded DNA, *Biochemistry 37*, 12496−12506.
49. Sugiyama, T., Zaitseva, E. M., and Kowalczykowski, S. C. (1997) A single-stranded DNA-binding protein is needed for efficient presynaptic complex formation by the Saccharomyces cerevisiae Rad51 protein, *J. Biol. Chem. 272*, 7940−7945.
50. Krejci, L., and Sung, P. (2002) RPA not that different from SSB, *Structure 10*, 601−602.
51. Bochkarev, A., and Bochkareva, E. (2004) From RPA to BRCA2: lessons from single-stranded DNA binding by the OB-fold, *Curr. Opin. Struct. Biol. 14*, 36−42.
52. Bujalowski, W., and Lohman, T. M. (1986) Escherichia coli single-strand binding protein forms multiple, distinct complexes with single-stranded DNA, *Biochemistry 25*, 7799−7802.
53. Kowalczykowski, S. C., Lonberg, N., Newport, J. W., and von Hippel, P. H. (1981) Interactions of bacteriophage T4-coded gene 32 protein with nucleic acids. I. Characterization of the binding interactions, *J. Mol. Biol. 145*, 75−104.
54. Berkowitz, S. A., and Day, L. A. (1974) Molecular weight of single-stranded fd bacteriophage DNA. High speed equilibrium sedimentation and light scattering measurements, *Biochemistry 13*, 4825−4831.
55. Kozlov, A. G., and Lohman, T. M. (2002) Stopped-flow studies of the kinetics of single-stranded DNA binding and wrapping around the Escherichia coli SSB tetramer, *Biochemistry 41*, 6032−6044.
56. Ralston, G. (1993) *Introduction to Analytical Ultracentrifugation*, Vol. I, Beckman Instruments, Inc., Fullerton, CA.
57. Maluf, N. K., and Lohman, T. M. (2003) Self-association equilibria of Escherichia coli UvrD helicase studied by analytical ultracentrifugation, *J. Mol. Biol. 325*, 889−912.
58. Lohman, T. M., and Mascotti, D. P. (1992) Nonspecific ligand-DNA equilibrium binding parameters determined by fluorescence methods, *Methods Enzymol. 212*, 424−458.
59. Lohman, T. M., and Bujalowski, W. (1991) Thermodynamic methods for model-independent determination of equilibrium binding isotherms for protein-DNA interactions: spectroscopic approaches to monitor binding, *Methods Enzymol. 208*, 258−290.
60. Kozlov, A. G., and Lohman, T. M. (1998) Calorimetric studies of E. coli SSB protein-single-stranded DNA interactions. Effects of monovalent salts on binding enthalpy, *J. Mol. Biol. 278*, 999−1014.
61. Lohman, T. M., Overman, L. B., and Datta, S. (1986) Salt-dependent changes in the DNA binding co-operativity of Escherichia coli single strand binding protein, *J. Mol. Biol. 187*, 603−615.
62. McGhee, J. D., and von Hippel, P. H. (1974) Theoretical aspects of DNA-protein interactions: co-operative and non-co-operative binding of large ligands to a one-dimensional homogeneous lattice, *J. Mol. Biol. 86*, 469−489.
63. Chrysogelos, S., and Griffith, J. (1982) Escherichia coli single-strand binding protein organizes single-stranded DNA in nucleosome-like units, *Proc. Natl. Acad. Sci. U.S.A. 79*, 5803−5807.
64. Brill, S. J., and Stillman, B. (1991) Replication factor-A from Saccharomyces cerevisiae is encoded by three essential genes coordinately expressed at S phase, *Genes Dev. 5*, 1589−1600.
65. Epstein, I. R. (1978) Cooperative and non-cooperative binding of large ligands to a finite one-dimensional lattice. A model for ligand-oligonucleotide interactions, *Biophys. Chem. 8*, 327−339.
66. Overman, L. B., Bujalowski, W., and Lohman, T. M. (1988) Equilibrium binding of Escherichia coli single-strand binding protein to single-stranded nucleic acids in the (SSB)65 binding mode. Cation and anion effects and polynucleotide specificity, *Biochemistry 27*, 456−471.
67. Bujalowski, W., and Lohman, T. M. (1989) Negative co-operativity in Escherichia coli single strand binding protein-oligonucleotide interactions. II. Salt, temperature and oligonucleotide length effects, *J. Mol. Biol. 207*, 269−288.
68. Kim, C., and Wold, M. S. (1995) Recombinant human replication protein A binds to polynucleotides with low cooperativity, *Biochemistry 34*, 2058−2064.
69. Blackwell, L. J., Borowiec, J. A., and Masrangelo, I. A. (1996) Single-stranded-DNA binding alters human replication protein A structure and facilitates interaction with DNA-dependent protein kinase, *Mol. Cell. Biol. 16*, 4798−4807.
70. Bochkareva, E., Korolev, S., Lees-Miller, S. P., and Bochkarev, A. (2002) Structure of the RPA trimerization core and its role in the multistep DNA-binding mechanism of RPA, *EMBO J. 21*, 1855−1863.
71. Yang, H., Jeffrey, P. D., Miller, J., Kinnucan, E., Sun, Y., Thoma, N. H., Zheng, N., Chen, P. L., Lee, W. H., and Pavletich, N. P. (2002) BRCA2 function in DNA binding and recombination from a BRCA2-DSS1-ssDNA structure, *Science 297*, 1837−1848.
72. Stauffer, M. E., and Chazin, W. J. (2004) Structural mechanisms of DNA replication, repair, and recombination, *J. Biol. Chem. 279*, 30915−30918.
73. Lohman, T. M., and Bujalowski, W. (1988) Negative cooperativity within individual tetramers of Escherichia coli single strand binding protein is responsible for the transition between the (SSB)-35 and (SSB)56 DNA binding modes, *Biochemistry 27*, 2260−2265.
74. Bujalowski, W., and Lohman, T. M. (1989) Negative co-operativity in Escherichia coli single strand binding protein-oligonucleotide interactions. I. Evidence and a quantitative model, *J. Mol. Biol. 207*, 249−268.
75. Nuss, J. E., Patrick, S. M., Oakley, G. G., Alter, G. M., Robison, J. G., Dixon, K., and Turchi, J. J. (2005) DNA damage induced hyperphosphorylation of replication protein A. 1. Identification of novel sites of phosphorylation in response to DNA damage, *Biochemistry 44*, 8428−8437.
76. Patrick, S. M., Oakley, G. G., Dixon, K., and Turchi, J. J. (2005) DNA damage induced hyperphosphorylation of replication protein A. 2. Characterization of DNA binding activity, protein interactions, and activity in DNA replication and repair, *Biochemistry 44*, 8438−8448.
77. Mass, G., Nethanel, T., and Kaufmann, G. (1998) The middle subunit of replication protein A contacts growing RNA-DNA primers in replicating simian virus 40 chromosomes, *Mol. Cell. Biol. 18*, 6399−6407.

78. Lavrik, O. I., Nasheuer, H. P., Weisshart, K., Wold, M. S., Prasad, R., Beard, W. A., Wilson, S. H., and Favre, A. (1998) Subunits of human replication protein A are crosslinked by photoreactive primers synthesized by DNA polymerases, *Nucleic Acids Res. 26*, 602−607.

79. Elmayan, T., Proux, F., and Vaucheret, H. (2005) Arabidopsis RPA2: a genetic link among transcriptional gene silencing, DNA repair, and DNA replication, *Curr. Biol. 15*, 1919−1925.

BI060994R